RETROGRADE TRANSPORT RATES IN THE G93A MOUSE MODEL OF AMYOTROPHIC LATERAL SCLEROSIS

by

Ingrid Johanna Lissel McFee
B.Sc. (Kinesiology), Simon Fraser University, 2003

THESIS SUBMITTED IN PARTIAL FULFILLMENT OF
THE REQUIREMENTS FOR THE DEGREE OF

MASTER OF SCIENCE

In the School of
Kinesiology

SIMON FRASER UNIVERSITY

Summer 2005

APPROVAL

Name: **Ingrid Johanna Lissel McFee**

Degree: **Master of Science**

Title of Thesis: **Retrograde Transport Rates in the G93A Mouse Model of Amyotrophic Lateral Sclerosis**

Examining Committee:

Chair: **Dr. Theodore Milner**
Professor, School of Kinesiology

Dr. Wade Parkhouse
Senior Supervisor
Professor, School of Kinesiology

Dr. Charles Krieger
Supervisor
Associate Professor, School of Kinesiology

Dr. Neil Watson
External Examiner
Associate Professor, Department of Psychology

Date Defended/Approved: July 8, 2005

SIMON FRASER UNIVERSITY

PARTIAL COPYRIGHT LICENCE

ABSTRACT

Amyotrophic Lateral Sclerosis is a late-onset, progressive neuromuscular disease involving degeneration of corticospinal tracts and motor neurons in the brain stem and spinal cord. Recently, it has been suggested that ALS results from a "dying back" axonopathy as opposed to originating in the motor neuron cell body. This is supported by a reduction of neuromuscular junctions in skeletal muscle prior to symptom onset and motor neuron death. It is known that there is a slowing of retrograde transport when comparing presymptomatic and end-stage mice; however, when during disease progression this occurs has not been clarified. By using a retrograde tracer, I sought to observe retrograde transport rates during disease progression in the G93A mouse, a murine model of ALS. Results indicate that retrograde transport is attenuated before symptom onset, loss of motor neurons, and precedes alterations in anterograde transport indicating this is one of the earliest pathological events in ALS.

ACKNOWLEDGEMENTS

I would like to thank my supervisory committee, Dr. Wade Parkhouse and Dr. Charles Krieger, for their support and guidance throughout my graduate career at Simon Fraser University. You have allowed me to work on a topic that I am extremely passionate about and develop a thesis that I am truly proud of. To Dr. Wade Parkhouse, I extend profound gratitude for being an excellent senior supervisor and mentor by allowing me to make my own mistakes – I have grown as a scientist and a person because of this. I would also like to thank the staff at the Animal Care Facility and in the Kinesiology main office for all their help and guidance as well as some much needed laughs.

To everyone at SFU that has helped make this experience a positive one – thank you. Whether you were ready with a much needed hug, running up a hill, or were trying to challenge me on a new level, it was much appreciated.

To my family, I could never begin to express how truly grateful I am and always will be for all the support you have provided me in so many ways. And to Ben, who has been my voice of reason and source of logic through this whole experience, I love you and thank you from the bottom of my heart.

TABLE OF CONTENTS

LIST OF FIGURES

LIST OF TABLES

CHAPTER 1: REVIEW OF LITERATURE

1.1 Introduction: Amyotrophic Lateral Sclerosis

Amyotrophic Lateral Sclerosis (ALS) is a rapidly progressive neurodegenerative disease that selectively attacks motor neurons in the motor cortex, brainstem, and spinal cord and thus has characteristics of both upper and lower motor neuron diseases (de Belleroche et al., 1995). Motor neurons may be targeted selectively due to their large cell bodies, long axons, and high level of mitochondrial activity (Hand & Rouleau, 2002). Generally, symptoms such as weakness and atrophy initially appear in the distal muscles of the arms and legs. Symptoms continue to progress and eventually the diaphragm and intercostal muscles become affected leading to respiratory failure usually within 3 to 5 years of symptom onset (Brown, 1995). Survival after symptom onset appears to depend on site of onset: individuals with onset affecting the limbs tend to have a survival rate of approximately 5 years, whereas individuals with bulbar onset tend to not survive as long. The disease affects between 1.2 and 1.8 in 100 000 people and is the most common neuromuscular disease, affecting people of all races but more men than women (Strong & Rosenfeld, 2003). The ratio of males to females in familial ALS is 1:1 but 2:1 in sporadic ALS although the ratio approaches 1:1 after the age of 60 (Haverkamp et al., 1995). ALS most commonly appears in people aged 50 to 60 years although there have been juvenile cases reported. Younger ages of symptom onset have been shown to have better survival outcomes.

1.1.1 Forms of ALS

Approximately 90 to 95 percent of ALS cases are deemed sporadic (sALS), meaning the disease occurs with no clearly associated risk factors such as a family history of the disease (Camu et al., 1999). The remaining 5 to 10 percent of cases are familial (fALS) resulting from an autosomal dominant pattern of inheritance. More specifically, around 20 percent of fALS patients carry a mutation in the Copper/Zinc superoxide dismutase 1 (SOD1) gene (Strong & Rosenfeld, 2003). This enzyme is an antioxidant that minimalizes damage caused by free radicals. Generally, the clinical features of sALS and fALS are indistinguishable which has lead to the hypothesis of a common final pathology. However, the age of onset in fALS is earlier at 46 years compared to at 56 years in sALS (Camu et al., 1999).

There is a rare, recessively inherited juvenile form of ALS with the age of onset in adolescence (Hadano et al., 2001). It is slowly progressing and has been linked to mutations in the gene for alsin, also called ALS2, which may be a guanine-nucleotide-exchange factor (GEF). GEF's act as the "molecular switch" in signal transduction pathways that affect the cytoskeleton as well as intracellular trafficking. Researchers have concluded that the loss of GEF activity causes the early-onset of this motor neuron disease (Yamanaka et al., 2003).

1.1.2 Sexual Dimorphism

There is pronounced difference in the number of males affected by ALS versus females. In sporadic ALS the ratio is 2 males: 1 female but as age passes 60 years the ratio approaches 1:1 (Haverkamp et al., 1995). This difference could be due to the longer

life expectancy of women although it has been speculated that sex hormones may play a role.

Weiner (1980) suggested that ALS may be a disease in which androgen receptors are down-regulated or non-functional. This could explain the male: female ratio and the sparing of cranial nerves III, IV, and VI which lack androgen receptors. More recently, it was shown that free testosterone levels were decreased in both male and female patients with ALS. Androgens are known to affect the morphology and survival of spinal cord and brain stem motor neurons as well as having an anti-apoptotic effect on cultured neurons (Forger et al., 1992; Pérez & Kelley, 1996). It has been speculated that this decrease in free testosterone levels may be due to an abnormal affinity of sex-hormone binding globulins (SHBG; Militello et al., 2002). Joseph and colleagues (1997) demonstrated that the overexpression of rat SHBG in transgenic mice lead to a rapidly progressive motor disorder characterized by hind limb paralysis.

It has also been observed that there are decreases in the serum concentrations of dehydroepiandrostone (DHEA), a neurosteroid, in ALS patients. DHEA-Sulphate (DHEAS) normally declines with age but has been shown to be lower than age-predicted concentrations in men with ALS. Women with ALS also had lower DHEAS concentrations but not as severe as men (Eisen et al., 1995). This suggests that the greater frequency of low serum levels of DHEA in males may play a part in their increased risk of ALS development (Eisen & Krieger, 1998).

Conversely, other researchers have suggested that it may be the female sex hormones that are neuroprotective and therefore delaying the onset of symptoms seen in women (Veldink et al., 2003; Czlonkowska et al., 2005, and Murashov et al., 2004)

although total survival time between sexes is not significantly different in animal models of ALS (Veldink et al., 2003). Estrogen may modulate cytokine expression discouraging inflammation, which plays a possible role in the pathogenesis of ALS. Pro-inflammatory cytokines have been shown to be elevated in ALS patients and animal models of the disease (Czlonkowska et al., 2005).

This hypothesis is contradicted by the observation that women on estrogen replacement therapy failed to have any benefits over women who were not receiving the hormone (Rudnicki, 1999). Interestingly, women receiving the hormone therapy had an earlier onset of symptoms suggesting that there was no clear evidence of a neuroprotective effect of exogenous estrogen in ALS. However, the administration of genistein, a phytoestrogen, to male transgenic SOD1 mice eliminated sexual dimorphism (Trieu & Uskun, 1999). In wild-type mice, the administration of 17β-estradiol significantly increased the retrograde transport rate in the sciatic nerve and administration of estrogen to ovarectimized females enhanced regeneration of the sciatic nerve after nerve crush injury (Murashov et al., 2004).

The evidence regarding the effect of sex hormones on the development of ALS is conflicting at best. However, as there are sex differences in the age onset and frequency of the disease, the idea of sex hormones conveying a susceptibility to the disease is not unreasonable. More research into the effect sex hormones have on the pathogenesis of the disease will clarify these ideas.

1.1.3 Pathology

Patients generally present with symptoms of both upper and lower motor neuron disorders. Spasticity and hyperreflexia, related to damage of the upper motor neurons, is accompanied by generalized weakness, muscle atrophy and eventual paralysis which occurs due to dysfunction and death of the lower motor neurons (Bruijn et al., 2004). Evidence of atrophy of the motor neurons and ventral roots as well as the shrinkage and discoloration of the lateral aspect of the lateral funiculi corresponding to the corticospinal tracts has been observed in ALS patients at autopsy (Brownell et al., 1970). Additionally, Wallerian degeneration of the remaining fibres has been documented (Delisle & Carpenter, 1984). There is a loss of motor neurons in the cranial nerve nuclei XII and motor nuclei of VI and VII in the brainstem as well as a loss of large Betz cells in the precentral cortex (Eisen & Krieger, 1998). Interestingly, there is a selective sparing of Onuf's nucleus (motor neurons that control the bladder) and motor neurons that control eye movements (Bruijn et al., 2004).

ALS tends to affect the motor neurons innervating muscles in the distal extremities (Eisen & Krieger, 1998). They are perhaps more vulnerable due to more extensive innervation by axons from the corticospinal tract (Eisen & Krieger, 1998). Death of motor neurons in the spinal cord is generally accompanied by reactive gliosis, intracytoplasmic neurofilament defects, and axonal inclusions containing organelles such as mitochondria and fragments of the small endoplasmic reticulum (Bruijn et al., 2004). Astrocytosis could have a buffering effect as they are involved in the uptake of glutamate and regulation of glutamate-induced excitotoxicity (Eisen & Krieger, 1998).

Skeletal muscle is atrophied and pale with angulated fibres (Eisen & Krieger, 1998). There is evidence of reinnervation with the loss of heterogeneity in terms of muscle fiber phenotype. The contractile characteristics of fast-twitch muscle have been shown to change in patients with ALS (Eisen & Krieger, 1998). Specifically, in the severe stage of motor neuron degeneration, alterations in the histochemical properties of muscle fibres show an increase in oxidative capacity. This results in a muscle such as the extensor digitorum longus (EDL) which is generally characterized as a fast-twitch muscle taking on the phenotype of a slow, fatigue-resistant muscle (Kieran et al., 2005).

1.1.4 Pathological Mechanisms

Jean-Martin Charcot first described ALS 136 years ago and the pathological mechanisms of ALS are still unclear. Although there are several prominent hypotheses involving environmental factors, mutations in Cu-Zn superoxide dismutase (SOD1), aberrant axonal transport, neurofilament aggregation, oxidative stress, and glutamate excitotoxicity, the precise mechanism remains elusive. More recently it has been postulated that hypotheses previously thought distinct may actually be interrelated and there may also be factors outside the nervous system involved in the pathological mechanisms (Strong & Rosenfeld, 2003). The idea of interrelated etiologies is supported by evidence indicating mitochondrial dysfunction, excessive oxidative damage, aberrant glutamate metabolism and the upregulation of microglial activity in ALS patients and mouse models.

The importance of delineating pathological mechanisms increases as larger proportions of our populations enter the most affected age brackets. However, the

increase in incidence of ALS can not solely be accounted for by the increase in the ageing populations, thereby renewing interest in environmental risk factors as possible initiators of the "pathological cascade" (Strong & Rosenfeld, 2003). Factors such as trauma, stress, or environmental exposure as pathological triggers remain speculative due to common predisposing factors (Strong & Rosenfeld, 2003). An exception to this is the Pacific or Guam variant of ALS. The incidence of ALS was found to be substantially higher in many villages of Guam but as the communities were westernised (including their diets) incident rates declined. It is postulated that the change in diet, most arguably sources of cycasin, and the correction of nutritional deficiencies, such as calcium and magnesium, contributed to this decline, thereby indicating that an environmental factor was contributing to the pathological mechanisms (Strong & Rosenfeld, 2003).

There is much to learn regarding the pathological mechanisms that result in the presentation of ALS. In order to better study these mechanisms scientists have purposefully altered breeding in lab animals to display certain phenotypes or altered certain genes to create models of the disease. The wobbler mouse and the progressive motorneuropathy mouse (pmn) are autosomal recessively inherited genotypes that develop motor neuron degeneration. The wobbler mouse is normal at birth but around 3-4 weeks develops slowly progressive motor defects within the forelimb (Eisen & Krieger, 1998). By 12-16 weeks death occurs due to severe muscle weakness. These animals display prominent vacuolization of the motor neurons within the brainstem and cervical spinal cord (Eisen & Krieger, 1998). The pmn mouse develops progressive paralysis of the hind limbs at around 3 weeks due to a mutation in a tubulin-specific chaperone protein which affects microtubule assembly within axons (Brommel et al., 2003). Hind

limb paralysis is followed by forelimb and brainstem involvement resulting in death by 6-7 weeks. This animal displays a "dying-back" motorneuropathy with distal axon degeneration and muscle atrophy without any attempted reinnervation (Eisen & Krieger, 1998). There are several transgenic models that can manifest in motor neuron degeneration that is characteristic of ALS. Three transgenic mice with mutant superoxide dismutase 1 (SOD1) genes have been studied extensively. The G93A, G85R, and G37R mice have a mutant human SOD1 protein that is expressed ubiquitously under the control of either a human or mouse SOD1 gene promoter (Bruijn et al., 2004). The mutation leads to a stable pattern of onset and progression: the onset of symptoms is characterized by weakness in the hind limbs from 3 to 12 months of age (depending on the mutation and on the copy number of the gene or the level it is expressed) and progresses to respiratory failure within a short time-period (Gurney et al., 1994). The onset of symptoms coincides with motor neuron loss, increased gliosis, and reactive microglia. The presence of ubiquitin-positive inclusions within the motor neurons and astrocytes has been observed in all three mutants (Dal Canto & Gurney, 1995).

1.1.4.1 Copper/Zinc Superoxide Dismutase (SOD1)

The enzyme SOD1 has been implicated in fALS via linkage analysis (Rosen et al., 1993). Currently, researchers have identified 90 mutations at 53 codons in all 5 exons of the SOD1 gene that affect both the primary and three dimensional structure of the protein (Shaw et al, 2003). SOD1 is a 16kDa protein that functions as a homodimer to scavenge free radicals and convert superoxide to hydrogen peroxide (Hand & Rouleau, 2002). Within the active site of each subunit is one atom of copper and one atom of zinc (Siddique & Deng, 1996). Superoxide is directed to the active site containing the copper

atom through a positively charged channel. The zinc atom serves to maintain the pH of the dismutation reaction and to aid in the rapid dissociation of hydrogen peroxide, which if accumulates can inactivate SOD1 (Siddique & Deng, 1996). Oxygen free radicals, such as superoxide anions and hydroxyl radicals, as well as reactive oxygen species such as hydrogen peroxide and nitric oxide are generated by metabolic reactions within the cell such as mitochondrial oxidative phosphorylation (Fullerton et al., 1998). SOD1 along with glutathione peroxidase catalase protect the cell from the excessive production of free radicals which can become highly toxic and disrupt normal cellular activity by interacting with membrane lipids, protein, and DNA (Fullerton et al., 1998).

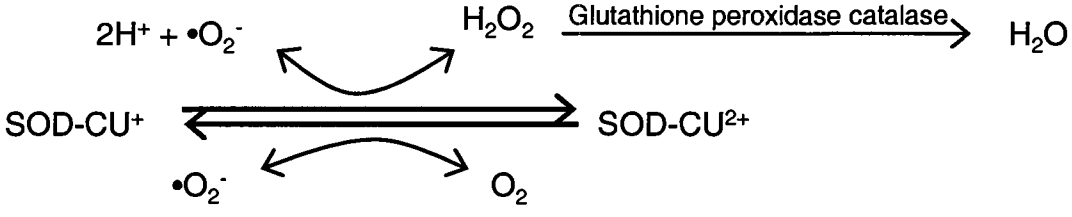

Observations have led to the hypothesis that fALS is not caused by a reduction or loss of SOD1 activity but instead to a "gain of function" that occurs independent of the level of SOD1 activity (Hand & Rouleau, 2002). This has been demonstrated through the production of SOD1 null mice which live to adulthood and do not develop motor neuron disease (Reaume et al., 1996). Additionally, the removal of normal SOD1 genes from transgenic mice that have had mutations introduced to the SOD1 gene so that it is dismutase inactive, did not result in a change of symptom onset or progression (Bruijn et al., 1998). It has been shown that the level of SOD1 activity does not correlate with disease onset or progression in animal models and in human patients (Cleveland et al.,

1995). Interestingly, increase in the levels of wild-type SOD1 and therefore dismutase activity has been shown to accelerate disease progression (Jaarsma et al., 2000).

The toxic gain of function could occur due to greater access of abnormal substrates to the active site or the mishandling of the copper and zinc ions (Bruijn et al., 2004). If a substrate other than superoxide is used, the production of peroxynitrite and hydroxyl radicals may occur. Peroxynitrite damages proteins by nitrating tyrosine residues (Beckman et al., 1994). This situation can occur when the reaction runs in reverse and oxygen is converted to superoxide which then combines with nitric oxide. The catalytic reaction can run in reverse if there is limited availability of zinc. The availability of zinc in cells is regulated by metalloenzymes, specifically metallothioneins (Bruijn et al., 2004). In the spinal cords ALS patients, metallothionein expression is upregulated (Nagano et al., 2001).

Initially, many scientists focussed their attentions solely on the motor neurons in the spinal cord. However, the mutant SOD1 is expressed ubiquitously in all tissues (Cleveland et al., 1995). The theory of non-cell autonomy is based on the idea that the environment of the motor neurons is significant, meaning other cells are involved in mitigating the damage sustained by the motor neuron (Cleveland et al., 1999). When mutant SOD1 was expressed only in astrocytes there was no development of motor neuron disease (Gong & Elliot, 2000) leading researchers to conclude that expression in astrocytes was insufficient to cause the disease. However, it has been shown that damage to the motor neurons requires mutation not only in the motor neuron but in the surrounding cells as well. In 2003, Clement and colleagues demonstrated that motor neurons expressing mutated SOD1 at levels that would cause early symptoms could be

rescued from degeneration and death if they were surrounded by normal nonneuronal cells such as astrocytes. Fischer and colleagues (2004) reported that reactive astrocytosis did not occur until 47 days of age (presymptomatic in the G93A transgenic mouse) and then progressed in intensity until death. Microglial activation did not occur at significant levels until after the onset of symptoms. These data indicate that the environment surrounding the motor neurons does have an impact; pathological mechanisms in the motor neurons alone do not cause the disease. Currently, phase III trials are being conducted on the use of Minocycline, an antibiotic that also blocks microglial activation. Minocycline has been shown to slow disease progression in mouse models of ALS (Kriz et al., 2002; Van Den Bosch et al., 2002; and Zhu et al., 2002).

Protein aggregation may occur when misfolded proteins combine to form insoluble inclusions. This occurs in several neurodegenerative diseases such as Alzheimer's disease (amyloid and tau) and Huntington's (huntingtin). Intracellular inclusions in the motor neuron and astrocytes have been seen in transgenic mice expressing SOD1 mutations and in human ALS patients (Bruijn et al., 1998). The disruption of the neurofilament light-chain gene in SOD1 mutant mice eliminates the assembly and accumulation of axonal neurofilaments and its subunits. This decreases the vulnerability of motor neurons to the toxicity mediated by misfolded SOD1 (Williamson et al., 1998). The question remains as to what damage these aggregates cause. It has been postulated that the aggregated proteins may lose function through their association with other aggregates (Bruijn, 2004). Other possibilities include the loss of protein-folding chaperones, dysfunction of the proteasome, the inhibition of organelles such as mitochondria, and the strangulation of the axon (Bruijn et al., 2004).

1.1.4.2 Neurofilament aggregation

Neurofilaments are the most abundant structural protein in motor neurons and are essential for the establishment of axonal diameter (Lee & Cleveland, 1996). The accumulation and abnormal aggregation of neurofilaments in the perikarya and proximal axon is present in sporadic and familial ALS as well as infantile spinal muscular atrophy and hereditary sensory-motor neuropathy (Bruijn et al., 2004). Collard and colleagues (1995) used a transgenic mouse model that overexpressed neurofilament proteins due to a variant allele of the neurofilament heavy-subunit gene which has been found in some ALS patients. The mouse showed progressive motor neurodegeneration with age due to neuronal atrophy and subsequent degeneration of axons distal to the neurofilament swellings. By injecting [^{35}S]-Methionine into the spinal cord, they showed that the retrograde transport of newly synthesised neurofilaments, tubulin, and actin was diminished. This resulted in the depletion of organelles in atrophied axons such as the filamentous structures, mitochondria, and small endoplasmic reticulum. They proposed that the neurofilament accumulation in the axons of this transgenic mouse resulted in axonal degeneration due to the impedance of the transport of key components in axonal maintenance. For example, a shortage of mitochondria could result in a severe disruption of energy metabolism.

The disruption of axonal transport due to neurofilament aggregation as a pathological mechanism is supported by several aspects of ALS. Motor neurons may be selectively vulnerable due to their high levels of neurofilament synthesis (Collard et al., 1995). Additionally, as slow axonal transport of cytoskeletal components is attenuated with age (Williamson & Cleveland, 1999), this increases the risk of abnormal

neurofilament aggregation in this population. In some familial ALS cases that were linked to SOD1 mutations, the presence of neurofilament accumulations as well as axonal swellings was evident (Collard et al., 1995). As mentioned previously, although there are several mechanisms that may result in ALS they may have a common pathological mechanism.

1.1.4.3 Aberrant axonal transport (Dynein)

Retrograde transport provides vital information to the cell body regarding the innervation status and environment of the axon terminals (Fischer et al., 2004). It has been shown that disruption of retrograde transport is sufficient to cause the degeneration of the motor neuron (Ligon et al., 2005). Dyneins are one of two families of microtubule motor proteins, the other family being the kinesins, and move cargo towards the minus end of microtubules. There are approximately 15 forms of dynein, the majority being involved in axonemal movement which refers to ciliary and flagellar movements (Vallee et al., 2003). There are only two forms of cytoplasmic dynein: cytoplasmic dynein 1 and 2. Cytoplasmic dynein 1 is ubiquitously expressed and plays a role in endoplasmic reticulum positioning, assembly of the mitotic spindle, nuclear and cellular migration and is the only known motor protein for retrograde transport (Bruijn et al., 2004). Dynein 2 is mainly limited to ciliated cells and has a narrower range of functions. The remaining discussion will focus on cytoplasmic dynein 1 which will be referred to simply as dynein.

Dynein is 1.2MDa multi-subunit complex consisting of a large heavy chain polypeptide (>500 kDa), that contains the ATPase and motor activities, and 3 types of accessory chains: intermediate, light-intermediate, and light (Vallee et al., 2003). The motor domain represents the majority of the heavy chain (350kDa) and is situated at the

C-terminus. It consists of a hexamer of ATPase subunits arranged in a ring, a shape which is highly conserved across species (Burgess et al., 2003). There are two projections from the motor domain, the 'stalk' is a 15 nm long structure that contains a microtubule-binding site and the 'stem' is the N-terminus of the heavy chain and is where the cargo binds (Vallee et al., 2003).

Dynein is associated with another protein complex, dynactin. Dynactin consists of 10 subunits including dynamitin and actin (Vallee et al., 2003). Its N-terminus region interacts with the intermediate chain of dynein. It is postulated that dynein is linked to its cargo through the p150 subunit of dynactin which is regulated by dynamitin (Hirokawa, 1998). By itself, dynactin is able to bind microtubules and disruption of the dynactin complex is sufficient to inhibit retrograde axonal transport (LaMonte et al., 2002). For example, a point mutation in the p150 subunit of dynactin causes a lower motor neuron disorder which begins with vocal cord paralysis (Puls et al., 2003). Dynein and dynactin together regulate retrograde transport and mediate neurofilament transport and stability at the neuromuscular junction (Ligon et al., 2005).

As proteins are manufactured in the cell body and then anterogradely transported towards the synapse, dynein faces a particularly challenging fate. It must be transported in the anterograde direction to function in retrograde transport. It has been shown that dynein is the only known motor protein responsible for retrograde transport (LaMonte et al., 2002). In studies that used nerve crush injuries or nerve ligation, dynein was found to accumulate in both the distal and proximal portion of the injury (Hirokawa et al., 1990). It has been shown that dynein can move bidirectionally along microtubules; however, it is unknown how it is able to switch directions once it reaches the synaptic ending of the

nerve. It has been postulated that activation and deactivation of dynein may involve phosphorylation and dephosphorylation (Hirokawa, 1998). Recently, an interdependence of the motor proteins has been demonstrated. If either kinesin or dynein is inhibited, there is a bidirectional block in the transport of vesicles along microtubules (Ligon et al., 2004). The light chain of kinesin binds to the intermediate chain of dynein, this interaction may be required to transport dynein to the periphery of the cell and to the axon terminal (LaMonte et al, 2002).

Another mouse model of neurodegeneration, the Loa model (Legs at Odd Angles) manifests late onset, progressive muscle atrophy due to the apoptotic loss of motor neurons (Hafezparast et al., 2003). When expressed, homozygotes die within 24 hours of birth due to an inability to move. Loa transgenic mice have a missense point mutation in the dynein heavy chain I gene which encodes the motor subunit of the protein. The mutation prevents dynein from dimerizing which is necessary for its activity (Andersen, 2003). The mutant acts in a dominant negative fashion as opposed to simply a loss of function. Hafezparast and colleagues (2003) proposed that the late onset of symptoms, presumably caused by motor neuron loss, may occur due to a compromise in retrograde transport resulting from an impairment in the dynein motor protein. This impairment would result in a decreased supply of trophic factors, such as IGF-1, GDNF, and CNTF, which are necessary for motor neuron survival.

When Kieran and colleagues (2005) crossed the Loa model with the G93A model they found that the hybrid had an increased lifespan of 28% and the onset of disease was delayed. The animals retained muscle strength for longer and had no changes in the contractile characteristics of fast-twitch muscle. There was increased motor unit and

motor neuron survival; however, consistent with the G93A mice, there was increased gliosis. They hypothesized that the rescue of motor neurons may be due to the mutation in dynein changing its interaction with SOD1, resulting in less dynein initially colocalizing with SOD1 aggregates. This may allow the proper transport of organelles such as mitochondria which could delay cell death.

As for dynein's involvement in ALS, as mentioned earlier the accumulation of neurofilaments creates a disease state similar to ALS and it is known that the retrograde transport of neurofilaments is dynein-dependent (Gurney, 1994). Additionally, mutations in the dynein system have been seen in human neurodegenerative disorders (Puls et al., 2003). Motor neurons are not the only structures vulnerable to defects in retrograde transport. Defects in dynein result in the attenuated retrograde transport of activated Trk receptor resulting in the degeneration of sensory neurons (Heerssen et al., 2004).

1.1.5 Apoptosis

Cell death due to the actions of mutant SOD1 is apoptotic occurring through caspase-mediated pathways (Rothstein et al., 1994). Apoptosis is programmed cell death which initiates a complex cascade of events that results in the non-inflammatory death of the cell (Gurney et al., 2000). The increase in free radicals that occurs from the expression of mutated Cu/Zn SOD1 results in the activation of caspase-1 and caspase-3. It has been shown that the activation of caspase-1 occurs months prior to neuronal death and the onset of symptoms (Pasinelli et al., 2000). Caspase-3 further propagates the process of cell death by acting on structural and maintenance proteins while caspase-1 promotes the production of IL-1β, a proinflammatory cytokine which increases the transcription of caspases and increases cell death (Gurney et al., 2000).

It has been speculated that investigation into the molecules responsible for preventing apoptosis, and their role in motor neuron death, may lead to the discovery of therapeutic interventions. However, Sagot and colleagues (1998) demonstrated that molecules that promote cell survival in a normal functioning system do not necessarily promote survival in a compromised system. Using a progressive motor neuronopathy (pmn) transgenic mouse, they demonstrated that retrograde axonal transport was reduced and while some neurotrophic factors (namely, ciliary neurotrophic factor (CNTF), brain-derived neurotrophic factor (BDNF), and neurotrophin-3 (NT-3)) were able to promote cell survival via a compensation for axonal deficiency, other neurotrophic factors (glial-derived neurotrophic factor (GDNF) and nerve growth factor (NGF)) could not. Previous experiments by Sagot and colleagues (1997) suggested that there may be two intracellular pathways involved in motor neuron degeneration; one that involves the cell body and another that involves axonal maintenance.

1.2 Retrograde Transport

A compromise in axonal transport has been found in many neurodegenerative diseases involving motor neurons, including human patients with ALS (Sasaki & Iwata, 1996). Axonal maintenance may play a key role in the pathological cascade of motor neuron diseases as demonstrated by findings that show when the first clinical symptoms in the pmn appeared there was no loss of motor neuron cell bodies, however, there was already an impairment in axonal transport (Sagot et al., 1998). Because the pmn model progresses much faster than the G93A mouse model of ALS, it is important to identify when axonal transport becomes compromised.

1.2.1 Methods of Studying Retrograde Transport

Retrograde transport is the movement of material from the axon terminal to the cell body. In the motor neuron that also involves the movement of materials from the neuromuscular junction up to the cell body. It is difficult to define a given motor neuron pool which is responsible for the formation of one particular nerve due to their dispersed localization within the ventral horn of the spinal cord (Haenggeli & Kato, 2002). This problem can be solved by the application of a retrogradely transported fluorescent dye or horseradish peroxidase (HRP) to a sectioned peripheral nerve or through an intramuscular injection (Mohajeri et al., 1998; Haenggeli & Kato, 2002). Traditionally, retrograde transport was studied by injecting HRP into an area and then examining its target after histochemical manipulation, usually with 3, 3'-diaminobenzidine (DAB; Schmued & Fallon, 1986). More recently, fluorescent dyes were employed, although they exhibited rapid fading, uptake by fibres of passage, limited cellular definition and diffusion of the dye from labelled neurons (Schmued & Fallon, 1986). In the 1980's Schmued and Fallon (1986) introduced the fluorescent tracer Fluoro-Gold. This stilbene has high commercial purity (99.2%) and a more intense emission spectra than other fluorescent labels. It has been shown that Fluoro-Gold is also compatible with immunohistochemistry (Ju et al., 1989) although there may be photobleaching due to the water content of select mounting media.

Fluoro-Gold conveys a bright gold fluorescence to the cytoplasm and lysosomes of labelled neurons, clearly defining the morphology of the cell body with extensive filling of the dendritic processes (Wessendorf, 1991). Once the tracer is internalized and retrogradely transported, it will not leak out of labelled cells despite prolonged survival

times because certain physical properties prevent the tracer from passively crossing the plasma membrane (Schmued & Fallon, 1986). It has been shown that when the retrogradely labelled neurons are axotomized and degenerate the persistence of small, brightly labelled cells occurs. This is not due to diffusion out of labelled neurons but due to the ingestion of the neurons by phagocytotic microglia within the spinal cord (Rinamen et al., 1991).

The precise mechanism of uptake at the neuromuscular junction is unknown but it is postulated that certain reactive groups, such as sugar moieties, may facilitate active endocytotic vesicular uptake into the axon terminal (Schmued & Fallon, 1986). This likely involves special invaginations on the plasma membrane called clathrin-coated pits that pinch off to form clathrin-coated vesicles containing extracellular fluid. The vesicles then shed their coat and fuse with the endosome. There would be some sorting mechanism and the endosome would be retrogradely transported to the cell body (Alberts et al., 1994). Results obtained from intramuscular injections of Fluoro-Gold could indicate whether the neuromuscular junction is still functional and whether the nerve terminal is capable of taking up the tracer (Haenggeli & Kato, 2002).

1.2.2 Defects in Retrograde Transport

Cellular components are synthesized in the cell body then transported down the axon to the synapse via both slow and fast transport (Bruijn et al., 2004). Components destined for the cell body (such as the target-derived growth factor NGF) are returned via fast retrograde transport mediated by the cytoplasmic motor protein dynein. Axonal transport is important in maintaining the morphological and functional integrity of motor

neurons. Diminished transport rates have been shown to be correlated with the development of motor neuron disease.

Williamson and Cleveland (1999) reported that transgenic mice with mutations in SOD1 (G37R and G85R) demonstrate slowed anterograde axonal transport prior to the onset of clinical symptoms and prior to any evidence of pathological changes. There are two forms of anterograde transport: Fast transport which is mediated by kinesin I and involves the transport of vesicles and mitochondria, and Slow transport which is mediated by an unknown mechanism and is responsible for the transport of major structural components, enzymes, and cytoplasmic proteins. Slow transport can be further broken down into SCa which occurs at approximately 0.5mm/day and moves neurofilaments, tubulin, and actin, and SCb which is slightly faster at 1-2mm/d and moves tubulin, actin, and other cytoplasmic proteins (Williamson & Cleveland, 1999). By injecting [^{35}S]-Methionine into the spinal cord they were able to observe the transport rates of all cargoes toward the axon terminal. Six months before symptom onset in both strains there was a significant attenuation in the transport rate of neurofilament and tubulin. Additionally, they found that tubulin transport was slowed by three months of age, which is nine months before symptom onset in these mouse models. By the end-stage of the disease axonal swellings were evident and displayed intense immunoreactivity for β_{III}-tubulin, a neuron specific isoform of β-tubulin. As might be expected some inclusions were also immunopositive for SOD1, but this was not a requirement for aggregation. These data demonstrate that the attenuation of slow axonal transport is a very early pathogenic event in the SOD1 transgenic mice.

LaMonte and colleagues (2002) demonstrated that the inhibition of retrograde axonal transport through a mutation in the dynein complex was sufficient to cause a late-onset progressive neuromuscular degeneration similar to ALS. It has been theorised that defects in axonal transport (both antero- and retrograde) may be the common pathway that results in the degeneration of motor neurons in ALS. Williamson and Cleveland (1999) proposed that the misfolding of the mutant SOD1 affects the transport machinery by causing a neurofilament accumulation and effectively "strangling" the axon. When the dynein complex was disrupted through an overexpression of dynamitin, and the affected animals were injected with Fluoro-Gold, there were no significant differences in retrograde transport rates in presymptomatic mice (LaMonte et al., 2002). However, even in mice displaying early symptoms the retrograde transport rate was significantly diminished although there were normal motor neuron numbers.

In a study by Mohajeri and colleagues (1998) they injected G1H mice (a variant of G93A) with a 4% Fluoro-Gold solution. Single injections into the medial gastrocnemius resulted in the labelling of a single well-defined cluster. Motor neurons innervating the medial gastrocnemius, lateral gastrocnemius, and soleus are located in the same motor column that is approximately 2 mm in length (Nicolopolouas-Stournas & Iles, 1983 as cited in Mohajeri et al., 1998). There is a mixture of large multipolar α-motor neurons with diameters of 19-37 μm and γ-motor neurons which are significantly smaller with denser and more evenly distributed labelling in the cytoplasm.

At 7 weeks of age (49 days) Mohajeri and colleagues found no significant difference between the number of α- motor neurons in the wild type versus the affected animals. However, by 9 weeks (63 days) there was a significant decline. By 18 weeks

(126 days) there was a 64% decrease in the number of α-motor neurons in the G1H mouse. The decrease in number was negatively correlated to disease progression. More specific time-points within disease progression were not investigated. They postulated that it might be possible that fewer motor neurons are labelled due to compromised axonal transport. However, they noted that while axonal transport may be deficient, it has not been studied directly. They also postulate that while retrograde labelling may be impaired, it was not sufficiently diminished to prevent any Fluoro-Gold labelling, as there were some motor neurons labelled with the same intensity level as the wild-type animals. This indicates that the deficits seen could be due to either a defect in the retrograde transport machinery or the neuromuscular junction.

1.2.3 Problems with the Retrograde Transport Machinery

Ligon and colleagues (2005) examined the G93A SOD1 mouse model of ALS, a model with predictable onset and progression of motor neuron degeneration, for defects in the dynein-dynactin system. They injected animals intramuscularly with Fluoro-Gold at several time-points and examined the lumbar spinal cord after 44 hours. They found that there was decreased labelling by 30 days that became statistically significant at 50 days. This suggests that neurodegeneration occurs relatively early and that slowed neurotracer uptake correlated temporally with decreased muscular strength (as assessed by grip-strength tests). They found no significant decrease in the expression of dynein or dynactin subunits but found that dynein colocalized with SOD1 aggregates. This could result in the misappropriation of active motor proteins. To investigate this further they examined primary motor neuron cultures in three conditions: uninfected, infected with HSV-LacZ, and infected with HSV-SOD1 (G85R). In the uninfected cells, dynein is

distributed throughout the cytoplasm and neurites, as it is in the HSV-LacZ cells. However, in the cells infected with HSV-SOD1 (G85R) dynein was found to be localized to large aggregates of SOD1. These data are evidence that SOD1 expression is sufficient to mislocalize dynein and to disrupt the integrity of the retrograde transport machinery.

In the G93A mouse model of ALS one of the earliest pathologies is a defect in slow anterograde transport (Williamson & Cleveland, 1999). This could result in the attenuated expression of dynein-dynactin at the neuromuscular junction. Early degeneration of the neuromuscular junction has been shown in this particular mouse model and the effects on retrograde transport must be considered.

1.2.4 Problems at the Neuromuscular Junction

Mitsumoto and colleagues (1990) examined retrograde transport in the wobbler mouse which inherits a lower motor neuron disorder through a recessive allele which primarily affects the forelimbs (Eisen & Krieger, 1998). Its major nerves are shorter in length than control animals and the retrograde transport rate is diminished in the cervical motor neurons but unchanged in the lumbar motor neurons (Mitsumoto et al., 1990). When animals were injected with HRP at 3 months of age, when the disease is unmistakable, there was reduced labelling of motor neurons that could be accounted for by a reduced amount of retrogradely transported materials. It is known that the intact neuron has basic rate of membrane turnover and therefore a basic rate of retrograde transport when the system is uncompromised (Bisby, 1977). The amount of retrogradely transported materials is a function of the rate of membrane turnover at the neuromuscular junction and will be affected by the degree of neuronal activity. This can be demonstrated by the increased amount of material transported after electrical stimulation

(Litchy, 1983) and the decreased amount of material transported after deafferentation (Peyronnard & Charron, 1983). In the wobbler mouse model there is only approximately 30% of cervical motor neurons remaining by 3 months; therefore, the decreased amount of retrogradely transported materials could be due to several factors. First, there may be a decreased number of intact neuromuscular junctions for the HRP to be taken up. Second, any vesicles containing HRP maybe returned to the sarcolemma in an attempt at axonal sprouting to reach the denervated endplates, thereby returning the HRP to the extracellular space. And third, the amount of material retrogradely transported may be reduced due to an impairment in fast anterograde transport resulting in decreased dynein to retrogradely transport the HRP.

The classical view of ALS is that the motor neuron cell body dies and then as a consequence, muscle weakness and death occur. However, recent research suggests that ALS may be a distal axonopathy, with a "dying back" pathophysiology in which distal axonal degeneration precedes neuronal degeneration and the onset of symptoms. Some studies have reported that dysfunction of the neuromuscular junction occurs at a time point before that of motor neuron loss (Fischer et al., 2004). Immunohistochemical analysis by Frey and colleagues (2000) showed the loss of neuromuscular synapses by day 50 (a presymptomatic stage) in the fast twitch muscles of G93A transgenic mice. Through electromyography, Kennel and colleagues (1996) reported the loss of motor unit numbers starting at age 40 days in the same model. Reports from Chiu and colleagues (1995) confirm this theory, stating that there is no significant loss of motor neurons in the G93A mouse spinal cord until the time of symptom onset.

Fischer and colleagues (2004) investigated disease progression in the G93A mouse. In their evaluation of 28 day mice they found no evidence of denervation in the medial gastrocnemius or axonal defects in the L4 ventral root. By 47 days of age there was a denervation of 40% of endplates but no corresponding change in the ventral roots. However, at 80 days, just prior to symptom onset, there were significant defects in the end-plates (~60% denervated) and a significant reduction in the number of axons in the ventral roots. It was only at this time point that vacuolisation of motor neuron cell bodies was observed. Clinical symptoms were not observed until after 80 days of age. The numbers of large motor neurons in the lumbar spinal cord did not decrease until between the 80 and 100 day time point, during when they decreased by 40%. Reactive astrocytosis was barely evident by 47 days but increased until death. Microglial activation was less prominent and did not occur until later time points. Fischer and colleagues concluded that before the loss of motor neurons occurs there is significant denervation of skeletal muscle resulting in the loss of neuromuscular junctions and a subsequent loss of ventral root axons. This indicates a progression of abnormalities from distal to proximal regions and thereby challenges the classical view of neuron dysfunction originating in the cell body. This further supports evidence of deficiencies in retrograde transport as a factor for initiating disease onset (Hafezparast et al., 2003; LaMonte et al, 2002; Puls et al., 2003). It was interesting to note that at 120 days there was an increase in the number of axons in the ventral roots as well as a shift to smaller axons in addition to an increase in the number of innervated neuromuscular junctions. This may represent a phase of compensatory regeneration of axons and reinnervation of

muscles that has previously be shown in SOD1 mice and in ALS patients (Bjornskov et al., 1984; Frey et al., 2000).

1.3 Retrograde Transport and Gene Therapy

Currently, there is no cure for ALS and treatments are aimed at slowing disease progression and improving patient quality of life. The drug Riluzole has had limited success. It was designed to block glutamate release but has been shown to increase motor neuron survival by stimulating the trophic activity of astrocytes (Peluffo et al., 1997). However, as there appears to be multiple factors contributing to the degeneration of motor neurons in ALS, a treatment that could save motor neurons from death in a generalized manner could potentially be useful to the wide range of ALS patients.

Trophic factors that are capable of promoting the survival of motor neurons have been an enticing candidate for treatment but unfortunately have had very little effect (Miller & Cleveland, 2003). Insulin-like growth factor I (IGF-1) has seemed a particularly viable candidate as serum IGF-1 levels are reduced in ALS patients suggesting an involvement of this system (Torres-Aleman et al., 1998). Administration of IGF-1 produced a mild slowing of disease progression in a North American clinical trial (Lai et al., 1997); however, a subsequent European trial yielded non-significant results (Borasio et al., 1998). Failures in previous efforts could be due to the method of delivery of IGF-1 to the motor neurons, as therapeutic uses of trophic factors could be limited by their short half lives or by toxicity (Boillee & Cleveland, 2004). While subcutaneous injections or even direct delivery into the cerebral spinal fluid provided disappointing results, Kaspar and colleagues (2003) have had success with viral delivery. In their experiments, Kaspar used an adeno-associated virus (AAV) to deliver IGF-1 to

the spinal cords of G93A mice (an animal model of ALS) via several intramuscular injections. The mechanism of therapeutic action involved the virus being taken up by the axon terminals in the muscle and retrogradely transported up the axon to the motor neuron cell body in the spinal cord. Once the virus reached the nucleus, the gene drove the production and subsequent secretion of IGF-1. It was found that the viral delivery of IGF-1 slowed the loss of spinal motor neurons, slowed forelimb paralysis and loss of hind limb strength, and increased life span by 5 weeks on average. Even if the injection was performed after the onset of symptoms, life span was increased by 3 weeks. It seems that the key to motor neuron survival involves the retrograde transport of the IGF-1 encoding virus, as injections of a variant of lentivirus encoding IGF-1 that could not be retrogradely transported had only a minor effect on extending survival (Kaspar et al., 2003). An interesting phenomenon occurred in this experiment: viral particles that were injected into the quadriceps had an effect on cervical motor neurons. Miller and Cleveland (2003) propose that perhaps the delivery of AAV-IGF-1 to the lumbar motor neurons stimulates the production of enough secreted IGF-1 to affect the cervical motor neurons. This may not be the case though as only 1.1% of the viral particles actually reaches the lumbar cord. Alternatively, when the virus is injected into the muscle some of the viral particles may enter the circulatory system and be delivered to cervical motor neurons (Miller & Cleveland, 2003).

Another promising study by Azzouz and colleagues (2004) reported that injections of a lentivirus carrying Vascular Endothelial Growth Factor (VEGF) delayed onset and slowed disease progression in the G93A mouse. They compared presymptomatic mice (21 days of age) with animals at the typical age of onset (90 days).

While they found that the older mice had fewer motor neurons that were transduced by the virus, they stated that this did not reflect a compromise in gene transfer efficiency (i.e. retrograde transport of the virus), instead they believe it reflects the smaller population of surviving motor neurons at disease onset. While this is supported by the findings of Dal Canto and Gurney (1995), the time point at which motor neuron death occurs, perhaps before the onset of clinical symptoms which would decrease gene transfer, was not investigated. Azzouz found that multiple injections (bilaterally into the gastrocnemius, diaphragm, intercostal, facial, and tongue muscles) into presymptomatic mice resulted in an increased life span of 30% when treated with VEGF. Additionally, the onset of symptoms was delayed by 40 days. In animals injected at the onset of symptoms, when many motor neurons have already died, there was increased survival of an average of 19 days longer than those injected with a control virus.

It is interesting to note that whatever the experimental model, neurotrophic factors do not affect the speed of retrolabelling in normal, control animals (Sagot et al., 1998). Possibly the rate of transport in these animals is already at an optimal level and can not be influenced by an exogenous source of factors. This supports the idea that normal or undamaged axons would not be capable of upregulating their retrograde transport mechanism in response to endogenous ligands. It is known that neurotrophic factors such as NGF induce changes in membrane structures (Connolly et al., 1979) and increase the number and velocity of transported particles on cultured neuronal cells (Yuki et al., 1996). It is also interesting that the application of neuronal and survival factors does not have an effect on wild-type animals. Perhaps there must be some compromise within the motor neuron before the exogenous neurotrophins are able to exert their effect.

While these results are encouraging, they are still based on injections at a time point that would not occur in human patients. The definite diagnosis of ALS rarely occurs immediately after symptom onset. Animal models that show the efficiency of viral vectors at a sufficient time after the onset of symptoms may have more external validity. Gene therapy in ALS works on the premise of delivering neuroprotective agents to the motor neuron cell bodies in the spinal cord. However, many researchers have proposed that axonal transport may be defective. Further questions arise as to the number of injections needed for effective treatment and the number of muscles to be injected. It has been shown that viruses can still promote gene expression 30 days after injection (Azzouz et al., 2004) but would they be able to continue for several years? As more research is done on this promising avenue of therapeutic intervention perhaps these questions will be answered.

CHAPTER 2: RETROGRADE TRANSPORT RATES IN THE G93A MOUSE MODEL OF AMYOTROPHIC LATERAL SCLEROSIS

2.1 Justification of Study

ALS is a progressive neuromuscular disease characterized by significant muscular atrophy and weakness. Diagnosis of the disease is difficult, as there are symptoms of both upper and lower motor neuron disorders that are characteristic of several other neuromuscular diseases. Since there are still no effective treatments or cures, once the disease is diagnosed only patient quality of life can be improved. Clinical trials involving the systemic administration of neuronal growth and survival factors (such as Insulin-like Growth Factor-1) have been disappointing (Lai et al., 1997; Borasio et al., 1998). There are conflicting reports as to the improvement in symptoms and increase in life span (Miller & Cleveland, 2003). Although IGF-1 promotes cell survival, it was unable to be transported to the motor neurons in the spinal cord via subcutaneous injections and direct delivery to the cerebral spinal fluid. However, if methods of improving retrograde transport in animal models could be established, more efficacious treatments could perhaps be discovered. As clinical signs do not usually appear until a large proportion of anterior horn cells have already degenerated, a treatment that involves improving retrograde transport within the axon as well as delaying motor neuron death would be advantageous.

There is now speculation that ALS may not originate in the cell body of the motor neuron but may be a "dying back" axonopathy originating in the distal axon. Studies

have shown that the neuromuscular junction is compromised well before both neurodegeneration and symptom onset. It has been shown that retrograde transport rates are significantly attenuated at the end-stage of disease in mouse models of ALS but when this attenuation occurs had yet to be identified. This study characterised the retrograde transport rates throughout disease progression in the G93A mouse and strengthens the hypothesis that ALS is a distal axonopathy.

2.2 Rationale

ALS remains an incurable and poorly treated disease with an unknown etiology. Although it is has been shown that retrograde transport in the G93A mouse is diminished, it is not known when during disease progression this occurs. Mohajeri and colleagues (1998) reported a decrease in the number of motor neurons labelled with Fluoro-Gold in G1H animals at 18 weeks of age. They postulated that it might be possible that fewer motor neurons are labelled due to compromised axonal transport. However, they noted that while axonal transport may be deficient, it has not been studied directly. They also postulate that while retrograde labelling may be impaired, it was not sufficiently diminished to prevent any Fluoro-Gold labelling, as there were some motor neurons labelled with the same intensity level as the wild-type animals indicating that similar amounts of Fluoro-Gold had been retrogradely transported.

As new hypotheses regarding ALS as a distal axonopathy emerge, it is imperative that the changes in retrograde transport during disease progression are identified as to assess the order of events in the pathological cascade. If motor neuron numbers are similar yet retrograde transport is attenuated, there may be a compromise in the distal axon or at the neuromuscular junction. This would indicate that the initial defect is in the neuromuscular junction or the axon, and precedes motor neuron degeneration and symptom onset. Thus, when quantifying the motor neuron pools in affected versus wild type animals there will be little difference in motor neuron numbers before symptom onset.

The benefits of viral based gene therapy can not be applied to human patients until, at minimum, symptom onset. As such, gene therapy must be able to improve motor

neuron survival after symptoms have appeared. An improvement in motor neuron survival and overall increases in life span relies heavily on the effective delivery of the virus or vehicle to the spinal cord. To identify the time-point during which the attenuation in retrograde transport occurs would be beneficial in determining how to adapt gene therapy protocols to overcome this slowing or even to find methods of ameliorating the defect. It is important to identify at which time point retrograde transport is diminished in order to further clarify the pathological mechanisms that result in Amyotrophic Lateral Sclerosis.

2.3 Objectives and Hypotheses

Experiment 1:

Objective 1

To characterize the retrograde transport rates of the neuronal tracer Fluoro-Gold as a function of disease progression in the G93A transgenic murine model of ALS.

Hypothesis

The retrograde transport rate will be attenuated in the G93A mouse compared with age-matched controls, with diminished amounts of materials transported as the disease progresses as indicated by smaller percentages of motor neurons displaying Fluoro-Gold.

Objective 2

To characterize the relative retrograde transport rates as function of symptomatology.

Hypothesis

The relative retrograde transport rates will decline before the onset of observable symptoms and continue to decline thereafter.

Experiment 2

Objective 1

To compare labelling at 24 hours and 72 hours after Fluoro-Gold injection to help elucidate factors that are contributing to alterations in retrograde transport rates.

Hypothesis

After 72 hours there will significantly more motor neurons labelled with Fluoro-Gold in the G93A mouse but it will still be significantly less than wild-type mice.

2.4 Methods

2.4.1 Animals

Transgenic mice expressing mutated human SOD1 gene were a generous gift from Dr. Charles Krieger. They correspond to the strain B6SJL-TgN (SOD1-G93A) 1Gur, which are available from The Jackson Laboratory and have been shown to model human fALS by overexpressing human Cu/Zn superoxide dismutase in which the 93rd residue, glycine, has been substituted with alanine (a mutation that has been found in cases of fALS, Gurney, 1994). The overexpression of SOD1 gene mutations in mice produces symptoms that are clinically and pathologically similar to amyotrophic lateral sclerosis in humans. It has been shown that agents active in slowing symptoms in this animal model have been predicative of clinical efficacy (Miller, 2001).

Mice were bred from progenitor stock animals and housed in the Animal Care Facility at Simon Fraser University. The colony was maintained by breeding affected males with unaffected (wild-type) females. Mice were weaned and genotyped at 28 days of age. Mice were classified as asymptomatic, mild, moderate, or severe based on a set of disease characteristic (see Appendix II for characteristics). Typically the onset of symptoms was 83 ± 5 days with death at approximately 130 days.

Mice are kept under a light cycle of 12 hours with dry food pellets and water available *ad libitum*. When mice manifested severe symptoms both food (in gel form) and water were available at several sites on the floor of the cage for easier accessibility. At no point were animals given any anti-inflammatory medication. Occasionally, animals at end-stage were given a low dose of pain medication, according to the advice of the Director of Animal Care, Dr. Madeleine Stephens (4 out of 5).

For the first experiment both control and affected mice were killed at several time-points: 55, 70, 85, 100, 115, and 130 days. For the second experiment, both affected and control mice were killed at 90 days of age (n=5). A total of 71 mice were sacrificed; 36 controls and 35 transgenic mice.

2.4.2 Determination of Animal Genotype

2.4.2.1 Polymerase Chain Reaction (PCR)

To prepare samples for the polymerase chain reaction (PCR) protocol, small ear tissue punches were immediately placed in an autoclaved 1.5 mL eppendorf tube along with 150 µl of Chelex solution to prepare the DNA template. The Chelex solution consisted of Chelex (5% w/v; Fluka, product #95577), Proteinase K (2µg/µl; Sigma Aldrich, product #P-2308), and RNase A (10µg/µl; Sigma Aldrich, product #R-4876). Tubes were then placed in a 55°C water bath for 15 minutes, vortexed for 10 seconds, and then immersed in the water bath for another 15 minutes. Tubes were vortexed for 10 seconds and then placed in a dry heating block set at 100°C for 8 minutes. Samples were vortexed for 10 seconds then centrifuged for 15 minutes at 12 000 rpm (Baxter Canlab Biofuge A). The supernatant from each sample was then transferred into a new, autoclaved eppendorf tube with autoclaved pipette tips (approximately 100µl). DNA templates were either used immediately as a template for the PCR protocol, or stored at -20°C.

PCR protocols adapted from Hu and colleagues (2003, for detail see Appendix A) were used to differentiate mice expressing the G93A transgene (affected) and those that did not (wild-type). Small volumes of PCR mixture were prepared (1.0µl DNA template, 0.5µl Primer mSOD1, 0.5µl Primer mSOD2, 0.5µl $MgCl_2$, 2.5µl of 10X buffer, 2.5µl of

dNTPs, 0.3µl Taq Polymerase, and 17.2µl of autoclaved distilled water; Qiagen, product # 201203). The primers used were: mSOD1 – CAT CAG CCC TAA TCC ATC TGA (forward) and mSOD2 – CGC GAC TAA CAA TCA AAG TGA (reverse). Both were obtained from Invitrogen. The dNTP stock solution (100mM) was made from individual dNTP solutions (Amersham, product # 27-2035-01) in the following volumes (10µl each of dCTP, dTTP, dATP, and dGTP with 460µl autoclaved, distilled water). To amplify the target transgene, the PCR was conducted using the following settings: 1 cycle for 5 minutes at 95°C; 30 cycles for 30 seconds each at 94°C, 56°C, and 72°C; 1 cycle for 30 seconds at 94°C and 56°C then 10 minutes at 72°C, the solution would then be cooled down to 4°C and kept there indefinitely. PCR protocols were run on a Gene Amp PCR System 2400 (Applied Biosystems).

2.4.2.2 Gel Electrophoresis

The PCR product was prepared for DNA electrophoresis by combining 2µl of loading dye with 10µl of sample. All 12µl of sample were loaded into a 1% w/v agarose gel (containing 0.01% Ethidium Bromide) along with positive and negative controls. Gels were run in a Mupid-21 Mini Gel Migration Trough (Cosmo Bio Co. Ltd) containing 0.5X Tris-Acetate-EDTA (TAE) buffer at 100V for approximately 30 – 45 minutes. Gels were then placed on a UV lamp (Fotodyne, Bio/Can Scientific) to determine the presence or absence of the mutant human SOD1 transgene (236 base pairs). If there was any questionable fluorescence (i.e. fragmented bands) samples were rerun to confirm genotype.

2.4.2.3 Determination of Symptomatology

The staff at the Animal Care Facility (ACF, Simon Fraser University) were informed as to which mice were affected (possessed the transgene) and which mice were wild-type. After 8 weeks of age, mice were routinely monitored (every second day) for the onset of symptoms according to various criteria such as bilateral flexion and muscle loss (as outlined in Appendix B) and then monitored daily. Other tests for mobility, body mass stability, hydration and hind limb splay were used to determine disease progression. The age at which symptom onset occurred as well as the symptomatology at the time the mice were euthanized was recorded.

2.4.3 Injection of Fluorescent Dye

Mice were anaesthetised in an induction chamber via a 5% Isofluorane flow. Once induced, they were maintained at a rate of 2-2.5%. Both affected G93A mice and age-matched controls were injected with 5μl of 2% Fluoro-Gold solution (in sterile saline; Fluorochrome Inc.) through a 1mm incision above the belly of the right gastrocnemius muscle using a 33-gauge needle connected to a 10μl gastight Hamilton syringe (#1702). The position of the syringe was controlled with a micromanipulator (see Figure 1). The 5μl injection occurred over a 2 minute period, the needle was then left in the muscle for 1 minute to prevent any tracer withdrawal via capillary action. The needle was then slowly withdrawn and polysporin was applied to the incision. Animals were taken off the anaesthetic and placed on 100% oxygen until they awoke. They then recovered under a heated lamp for 30 minutes before being placed back in their original cages. Animals further recovered for 24 hours for the first experiment and 72 hours for the second experiment, and were then euthanized with a CO_2/O_2 mixture. After they had

stopped breathing but before cardiac arrest, they were perfused transcardially with 30 mL of 1X Phosphate buffered saline (pH 7.4) followed by 30 mL of 4% paraformaldehyde (pH 7.4; Sigma Aldrich, product #P6148) at room temperature. The spinal column from the lower thoracic to sacral region and both the left and right gastrocnemius were then removed and further fixed in 4% paraformaldehyde over night. The lumbar spinal cord was then dissected out and fixed for another 2 hours. Both the spinal cord and gastrocnemius were then cryoprotected in 20% sucrose (w/v in 1X Phosphate buffered saline) for 24 hours.

2.4.4 Immunohistochemical Analysis

2.4.4.1 Cryosectioning

The lumbar spinal cord was mounted in optimal cutting temperature (OCT) medium (Tissue Tek) and sectioned transversely on a Reichert-Jung Cryocut 1800 (Leica) using Feather microtome blades (Tissue Tek). Sections were cut at 30μm then placed in 1X PBS for further processing. Sections were cut when the cryostat was at 15-17°C.

2.4.4.2 Immunofluorescent Staining

Although Fluoro-Gold is deemed non-toxic, unilateral injections were employed to serve as an internal control. To exclude the possibility that some motor fibres were in the process of degenerating and thus could not take up the FG after the injection, I counterstained the sections with Choline Acetyltransferase (ChAT) and examined motor neurons on both sides of the spinal cord. There were no significant differences between the numbers of ChAT-stained motor neurons bilaterally. ChAT is the enzyme

responsible for the biosynthesis of acetyl choline and is presently the most specific marker for the identification of cholinergic neurons in both the central and peripheral nervous system (Ona & Nakanishi, 2000). It is present in neurons in the basal forebrain, striatum, cerebral cortex, mesopontine tegmental nuclei, cranial motor nuclei, and spinal motor neurons.

Free floating 30μm sections were counterstained with antibodies to ChAT in order to identify motor neurons in the sciatic pool (for full protocol see Appendix C). Briefly, sections were rinsed in 1X PBS then incubated for 1 hour in a blocking solution containing 2% Normal Donkey Serum and 5% Bovine Serum Albumin at room temperature. The sections were incubated in the primary polyclonal antibody (1:200, goat anti-ChAT; Chemicon International) for approximately 48 hours at 4°C. After several washes with 1X PBS, the sections were incubated in the secondary antibody for 1.5 hours at room temperature in absence of light (1:400, donkey anti-goat Alexa Fluor 555; Molecular Probes).

After several washes with 1X PBS, sections were mounted on glass slides (Fischer Scientific) and air-dried in the absence of light. Once dry, a small amount of Vectashield Mounting Medium for Fluorescence (Vector Laboratories Inc.) was added to the slide before carefully applying cover-slips. Cover-slips were sealed with clear nail-polish. Slides were then stored in the absence of light at 4°C. Several slides were made containing sections that had only been labelled with the secondary antibody to serve as controls when determining auto-fluorescence during the imaging process.

2.4.4.3 Imaging

Sections were visualised using an Olympus BHX40 wide-field epifluorescent microscope. A U-MWU2 wide-band UV filter (excitation filter: 330-385, emission filter: 420; Olympus) was used for Fluoro-Gold imaging (excitation: 360 nm, emission peak: 620 nm.) and a U-MWIG wide-band cube filter (excitation filter: 530-550, emission filter: 570nm, Olympus) was used for Alexa Fluor 555 imaging (excitation: 555 nm, emission peak: 565 nm). Images were acquired through a CoolSnap CCD camera (RS Photometrics) and processed with MetaVue 4.6 software (Universal Imaging Corp). Images were collected at 10X (NA=0.25), 20X (NA=0.40), and 40X (NA=0.75). Sections collected at 40X were used for the counting of ChAT-positive and Fluoro-Gold-positive cells. All images were collected under constant conditions (1ms exposure time, brightness, and contrast[1]) in order to limit variability for assessment purposes. Background fluorescence levels were determined for ChAT using several sections only exposed to secondary antibodies and averaging the intensity levels. It was found that the blocking procedure had been sufficient to negate the removal of the background fluorescence. For Fluoro-Gold, the use of the wide-band UV filter did not allow us to properly remove background fluorescence.

2.4.4.4 Image Analysis

In all sections, the anterior ventral horn of the lumber spinal cord was examined. Motor neurons of the sciatic pool were identified as neurons in lamina IX in the region of L3 to L6 ipsilateral to the Fluoro-Gold injection. Using the criteria set by Mohajeri and colleagues (1998), Fluoro-Gold-labelled motor neurons were identified by the presence

[1] Fluoro-Gold: brightness levels were kept between 50-55% and contrast levels were kept between 70-75%. ChAT: brightness levels were kept between 50-55% and contrast levels were kept between 65-70%.

of staining confined to the cytoplasm with a clear nucleus that is devoid of staining. In older affected mice (specifically 115 – 130 days) there was often the presence of Fluoro-Gold in the cytoplasm without the clear nucleus. Alternate channels were checked for bleed-through, and upon this confirmation were counted as a Fluoro-Gold-positive cell. This type of staining was not found in the wild-type sections, nor in the G93A sections at earlier time-points. The lack of a clearly defined nucleus could be indicative of a dying motor neuron, as is consistent with these time-points (Mohajeri et al., 1998) but more likely is due to the level of intensity. Schmued and Fallon (1986) showed figures of neurons displaying intense Fluoro-Gold staining in which the nucleus was not clearly defined. ChAT-positive cells were identified as those displaying extensive staining around the cell surface and often within the cytoplasm. Representative images of Fluoro-Gold positive cells, ChAT-positive cells, and the overlaid image are demonstrated in Figure 2.

The sciatic motor neuron pool extends approximately 2mm longitudinally in the lumbar spinal cord. As sections were cut at 30μm, every fourth section was analyzed to avoid the double-counting of motor neuron cell bodies which can reach up to 100μm in length. This yielded a possible 16 sections to analyze. Eight sections were chosen at random for analysis and the number of Fluoro-Gold-positive and ChAT-positive cells was assessed and recorded. Motor neurons innervating the medial gastrocnemius were consistently found in the dorsolateral region of the anterior ventral horn (Figure 2). Sections were counted blind to genotype and time-point. The percentage was then calculated for each section and averaged across the eight counted to yield a final percentage of motor neurons displaying Fluoro-Gold. By analyzing the percentages

based on a 24 hour time-period I can hypothesize about the relative retrograde transport rates and the effect disease progression has on them.

2.4.5 Data Analysis

2.4.5.1 Animals

G93A mice were age-matched to wild-type controls and euthanized at day 55, 70, 85, 100, 115, and 130. The mean body mass and the mean percentage of motor neurons displaying Fluoro-Gold were calculated for each group. Data was analyzed for normality via residual plots and the Shapiro-Wilks test, prior to further analysis. The Shapiro-Wilks test was significant ($p = 0.015$); therefore, the null hypothesis was accepted and non-normality was assumed. Consequently, the weight data points were log transformed which yielded a non-significant Shapiro-Wilks test ($p = 0.054$). Independent t-tests (two tailed) were used to compare means between G93A affected mice and wild-type controls at each time-point. An α-level of 0.05 was set as significant for all tests and all results are reported as mean $\pm$ standard deviation, unless otherwise stated. A two-way 2 (disease) X 6 (time-point) randomized group ANOVA was used to compare weights between G93A mice and wild-type mice. Tukey's post hoc tests were used to examine individual group differences among the data. The mean age of symptom onset was calculated based on the age at which animals first began showing symptoms based on a criteria set by the staff at the Animal Care Facility (see Appendix B).

In the second experiment, data was collected using both G93A and wild-type mice at 90 days of age. These animals underwent the same injections as the previous experiment but were euthanized after 72 hours. An independent samples t-test was used to assess differences in mean body mass.

2.4.5.2 Immunohistochemistry

The mean percentage of motor neurons displaying Fluoro-Gold data was assessed for normality prior to further analysis using residual plots and the Shapiro-Wilks test. The Shapiro-Wilks statistic ($W = 0.990$) non significant ($p = 0.89$); therefore, the null hypothesis was rejected indicating that the data had a normal distribution. To confirm that there was no significant age-effect associated with the mean percentage of motor neurons displaying Fluoro-Gold in the wild-type spinal cords, a one-way ANOVA was conducted for wild-type animals across time-points. Since no significant difference was found between wild-type samples ($p = 0.175$), a two-way 2 (disease) by 6 (time-point) randomized groups ANOVA was conducted to compare the group means of the percentage of motor neurons displaying Fluoro-Gold. Tukey's post-hoc tests were performed to examine the differences among the time-points. Independent t-tests were used to compare means between G93A and wild-type mice at each time-point. The mean number of ChAT-positive and Fluoro-Gold-positive motor neurons were calculated and then analyzed separately using a 2 (disease) by 6 (time-point) randomized groups ANOVA. G93A mice were then grouped according to the symptoms exhibited at the time of euthanasia and the mean percentages of motor neurons displaying Fluoro-Gold were compared against each other as well as against wild-type mice with a one-way ANOVA.

The mean percentage of motor neurons displaying Fluoro-Gold collected from the second experiment was analyzed using an independent t-test between the G93A and wild-type animals at 90 days of age. These data were also compared to a similar time-point (85 days) in which data was collected 24 hours after the Fluoro-Gold injection: wild-type

after 72 hours (WT_{72}) vs. wild-type after 24 hours (WT_{24}) and G93A after 72 hours ($G93A_{72}$) vs. G93A after 24 hours ($G93A_{24}$). The mean percentage of motor neurons displaying Fluoro-Gold were compared using a 2 (disease) by 2 (time after injection) randomized groups ANOVA. The mean number of ChAT-positive and Fluoro-Gold-positive motor neurons was calculated for both times and a 2 (disease) by 2 (time after injection) randomized groups ANOVA was run for each group of cells.

2.5 Results

2.5.1 Animals

Mean body mass was significantly different across time-points ($F_{5,49}$ = 9.613, p<0.001) and across genotype (disease; $F_{1,49}$ = 55.733, p<0.001). However, these differences were not constant as there was a significant time-point by disease interaction effect ($F_{5,49}$ = 3.749, p = 0.006). There was a general trend that the difference in mean body mass between wild-type and G93A mice increased over disease progression. Specifically, the mean difference in body mass between 55 days of age and 70 days of age (p<0.005) was significant. However, from day 70 onwards although there was an increase in the mean difference, the incremental increases themselves were not significantly different from each other.

The mean body mass of G93A and wild-type mice was not significantly different at 55 days of age. However, at all time-points thereafter, the G93A mice had body masses that were significantly less than wild-type controls as is summarized in Figure 3 (day 70: 24.5 ± 1.6g vs. 27.4 ± 0.8g respectively; p = 0.014, day 85: 23.8 ± 2.3g vs. 30.0 ± 1=3.0g; p = 0.017, day 100: 22.0 ± 2.7g vs. 28.8 ± 4.8g; p = 0.031, day 115: 19.0g ± 2.2g vs. 25.1 ± 2.6g; p = 0.004, day 130: 17.4 ± 2.1g vs. 26.0 ± 3.2g; p<0.001). There was a significant sex effect on weight (p<0.001).

It was determined, using a Shapiro-Wilks test, that the data for the age of symptom onset was normally distributed (W = 0.941, p = 0.337). Although there was considerable variability in the age of onset of symptoms (range: 65 – 96 days), a one-way ANOVA found that there was no significant difference in the mean age of onset of

symptoms across time-points. The overall mean age of symptom onset was 83 days ± 9 days. There was no significant sex effect.

The normality of the body mass data for the second experiment was confirmed with the Shapiro-Wilks test (W = 0.903, p = 0.300). The mean body mass for wild-type mice at 90 days, 72 hours after the Fluoro-Gold injection was 20.4 ± 2.3g and for G93A affected mice was 20.8 ± 2.0g. There was no significant difference in body mass between the two genotypes at 90 days of age.

2.5.2 Immunohistochemistry

The mean percentage of motor neurons displaying Fluoro-Gold as a measure of relative retrograde transport rates was significantly different across time-points ($F_{5,49}$ = 18.182, $p<0.001$) and across genotype (disease; $F_{1,49}$ = 160.81, $p<0.001$). However, this difference was not constant as indicated by a significant time-point by disease interaction effect ($F_{5,49}$ = 20.715, $p<0.001$). In the G93A mice, there was a significant decline in the percentage of motor neurons displaying Fluoro-Gold from day 55 to day 70 and then a plateau until day 115 when there was again a significant decrease. This was supported by results from Tukey's post-hoc test: in the G93A mice the mean difference in the percentage of motor neurons displaying Fluoro-Gold between 55 and 70 days of age was significant ($p<0.05$) and the mean difference between mice at 115 days of age and 130 days of age (p = 0.004) was significant. Individual t-tests between G93A and wild-type mice at each time-point revealed that at day 70 and onwards G93A mice had significantly lower percentages of motor neurons labelled with Fluoro-Gold, as shown in Figure 4 (values reported as G93A vs. wild-type; day 70: 63 ± 4% vs. 84 ± 6%; p = 0.001, day 85: 60 ± 9% vs. 77 ± 5%; p = 0.027, day 100: 57 ± 13% vs. 82 ± 5%; p = 0.008, day 115: 51

± 11% vs. 84 ± 6%; p = 0.002, day 130: 16 ± 16.% vs. 86 ± 6%; p<0.001). Images representative of those counted are displayed in Figures 5 and 6.

Data was further analysed and separated into the average number of ChAT-positive motor neurons and Fluoro-Gold-positive motor neurons counted per animal (summarized in Table 1). From each animal, eight sections at random were analyzed. It was found that averaged over the time-points, G93A mice had significantly fewer ChAT-positive motor neurons than wild-type (63 ± 15 vs. 80 ± 15, p<0.01). Specifically, G93A mice had significantly fewer ChAT-positive motor neurons at 55, 70, and 130 days of age (p<0.04). As expected, when comparing the Fluoro-Gold-positive motor neurons, it was found that average over time-points G93A mice had significantly fewer labelled cells than wild-type mice (35 ± 19 vs. 66 ± 15, p<0.001). When comparing genotypes at the different time-points it was found that at all time-points except 85 days, G93A mice had significantly fewer Fluoro-Gold-positive cells (p<0.02).

When G93A mice were grouped according to the symptoms exhibited at the time of euthanasia and were compared against other symptom groups and wild-type controls, there was a significant difference in the mean percentage of motor neurons displaying Fluoro-Gold between symptom groups ($F_{4,56}$ = 44.000, p<0.001). The mean percentages are reported in Table 2. When comparing wild-type mice to G93A mice it was found that the mean percent of MN displaying FG was significantly different at all symptom groups (wild-type (84 ± 6%) vs. no symptoms (72 ± 12%): p = 0.041, mild (59 ± 8%): p<0.001, moderate (49 ± 15%): p<0.001, severe (26 ± 24%): p<0.001). Although there is a general decrease in percent of motor neurons displaying Fluoro-Gold across symptoms, it was found that there was no significant difference between G93A mice showing no symptoms

and those showing mild symptoms. The general trend indicates there is a significant decline in Fluoro-Gold-labelled cells from wild-type to G93A no symptoms ($p<0.05$) and subsequently there is a gradual decrease from no symptoms to mild to moderate symptoms (although it is non-significant) with a final significant decline at the severe stage of the disease ($p<0.01$).

For the second experiment, after normality was confirmed using the Shapiro-Wilks test ($W = 0.863$, $p = 0.089$) an independent t-test (two-tailed) was run to assess the difference in the mean percentage of motor neurons displaying Fluoro-Gold. It was found that at this 90 day time point, 72 hours after the Fluoro-Gold injection there was no significant difference between the G93A and wild-type mice ($80 \pm 12\%$ vs. $87 \pm 4\%$ respectively; $p = 0.303$, see Figure 7). When comparing these values to animals euthanized after 24 hours at a similar time-point (85 days) it was found there was a significant increase in the percentage of motor neurons displaying Fluoro-Gold in both the wild-type and G93A mice ($p<0.03$; as shown in Figure 8).

When data was analyzed by looking at the number of ChAT-positive and Fluoro-Gold-positive cells there was an interesting result (as shown in Figure 9). As expected, there was no significant difference in the number of ChAT-positive cells in both the wild-type and G93A mice when compared at 24 hours versus 72 hours. However, although was an increase in the number of Fluoro-Gold labelled cells in wild-type mice (WT_{24} versus WT_{72}) the results were non significant. There was a significant difference in the number of labelled cells in G93A animals ($G93A_{24}$ versus $G93A_{72}$: 43 ± 14 vs. 74 ± 7, $p<0.01$). This is in contrast to the finding that in both wild-type and G93A mice there is

a significant increase in the percentage of motor neurons displaying Fluoro-Gold when comparing the 24 hour and 72 hours time-points ($p<0.03$).

2.6 Discussion

Until recently, the contributions of distal regions of the axon, such as the neuromuscular junction, to motor neuron degeneration have been discounted as possible pathological triggers. For example, Azzouz and colleagues (2004) observed that in the G93A mouse at symptom onset fewer motor neurons were transduced by an intramuscularly injected lentivirus. They stated that the decrease was not a reflection of a compromise in retrograde transport but instead was due to a decrease in the population of surviving motor neurons. However, alterations in retrograde transport have been shown to have deleterious effects on the survival of neurons in both the peripheral and central nervous system. In ALS patients, impaired axonal transport and axonal abnormalities have been observed in spinal motor neurons. In animal models, it has been shown that the disruption of retrograde transport can result in motor neuron degeneration that is characteristic of ALS. Specifically, in the G93A transgenic mouse, changes in retrograde transport have been observed between presymptomatic stage and end-stage mice, but the changes in retrograde transport as a function of disease progression have not yet been examined.

In this study I examined the retrograde transport rate of the sciatic nerve in the G93A mouse model of ALS throughout disease progression. I injected the neuronal tracer Fluoro-Gold into the right medial gastrocnemius of G93A mice and age-matched controls at various time-points throughout disease progression. The animals were sacrificed 24 hours later and their lumbar spinal cords examined. The number of Fluoro-Gold labelled cells, identified by criteria set by Mohajeri and colleagues (1998), were calculated as a percentage of ChAT-positive cells, and these values were used as an

indication of retrograde transport rate. As hypothesized, I found that retrograde transport rates are attenuated before the onset of clinical symptoms. Specifically, they are diminished by 70 days of age, a time-point which occurs before the reported loss of motor neuron cell bodies (Chiu et al., 1995). These results suggest that the pathological trigger for neurodegeneration may involve the distal axon via impairment in the uptake capacity of axonal terminals or the ability to retrogradely transport key components in motor neuron survival.

G93A transgenic mice: a model of ALS

Transgenic mice have been developed to study diseases in which there is a genetic component. These animals are constructed by incorporating and manipulating specific genes so that a certain disease phenotype will be expressed. The G93A transgenic mouse is manufactured by introducing mutant human superoxide dismutase genes (SOD1) that have a point mutation at the 93rd residue where glycine has been switched to alanine resulting in the development of a disease that is clinically and pathologically similar to ALS. There is vacuolar degeneration of motor neurons in the anterior ventral horn leading to the atrophy of axons, the deposition of neurofilamentous inclusions and the loss of cell bodies. This model is one of most commonly used when studying ALS and has been well-characterized. The animals undergo progressive denervation of distal muscles with progressive neurodegeneration, leading to muscle atrophy and weight loss, ultimately resulting in death due to respiratory failure at approximately 130 days of age.

At 55 days of age there was no difference in the body mass of G93A mice versus age-matched wild-type mice. Both groups had increased in body mass by day 70, which may correspond to a period of maturation. However, G93A mice did not experience the

same weight gain as controls (see Figure 1). From day 70 onwards there was no change in the weight of wild-type mice; however, G93A mice gradually lost weight until at 130 days of age they were at 71% of their peak weight. These values are similar to those obtained previously (Cunningham, 2005; Chiu et al., 1995; Gurney et al., 1994, Fischer et al., 2004). The diminished weight of the G93A mice at 70 days is coincident with reported denervation-induced atrophy observed in the triceps surae (Fischer et al., 2004; Frey et al., 2000). Additionally, the 30% drop in body weight is larger than what has been reported elsewhere. Chiu and colleagues (1995) reported only a 20% decline; however, this discrepancy may be due to the use of both males and females in this study as there was a significant effect of sex on mean body mass.

The average age of symptom onset was 83 ± 9 days. While this corresponds with data previously collected in our laboratory (Cunningham, 2005) it is lower than what the majority of literature reports (~90 days: Millecamps et al., 2001; Chiu et al., 1995; Frey et al., 2000; Gurney et al., 1994). Transgenic expression levels have been shown to correlate with neurotoxicity and mice with a higher copy number exhibit earlier ages of onset (Alexander et al., 2004). A change in the transgene copy number may occur during mating due to an intra locus recombination during meiosis (Gurney, 1997). While the age of onset in the present study may be earlier, there are several G93A strains that present symptoms later (Mohajeri et al., 1998; Williamson & Cleveland, 1999; Feeney et al., 2001) presumably due to a lower transgene copy number. The range in the age of symptom onset is large (65-96 days) which may be due to the use of both males and females in this study. Veldink and colleagues (2003) reported that the onset of symptoms was earlier in males but females did not have increased survival periods.

Changes in the percentage of motor neurons displaying Fluoro-Gold

Animals were given a single intramuscular injection of Fluoro-Gold and sacrificed 24 hours later. It was found that the percentage of ChAT-positive motor neurons displaying Fluoro-Gold in G93A mice was already significantly attenuated compared to wild-type animals by day 70. The percentage of motor neurons labelled with Fluoro-Gold remained constant in the wild-type mice throughout all time-points; however, in the G93A mice, the percentage dropped significantly from 55 to 70 days with a plateau until 115 days followed by another significant decline. When comparing animals based on their symptomatology at the time of death, the percentage of motor neurons labelled with Fluoro-Gold was significantly lower in all G93A groups (no symptoms, mild, moderate, and severe symptoms) compared to wild-type mice. Although there was a significant sex effect observed in weight, this was not observed in the onset of symptoms nor in the percentages of motor neurons labelled with Fluoro-Gold. The difference initially observed between wild-type and G93A mice with no symptoms was exacerbated as the disease progressed with the percentage of motor neurons labelled with Fluoro-Gold in mice with severe symptoms being 50 points less than mice with no symptoms. These results agree with our hypothesis that in the G93A mice, retrograde transport rates would be diminished before the onset of observable symptoms.

In animal models of ALS, it has been shown that neuronal dysfunction precedes the clinical onset of symptoms. It has also been shown that extensive nerve sprouting and synaptic remodelling occurs as part of the compensatory reinnervation process (Feeney et al., 2001). Fischer and colleagues (2004) reported that before any loss of motor neurons

there is a severe loss of ventral root motor axons and preceding this there is significant denervation at the corresponding neuromuscular junctions. These results indicate that there are defects at the neuromuscular junction and within the axon before symptom onset which could account for the differential pattern of retrograde transport rates throughout disease progression. A biphasic pattern of a steep loss followed by a plateau, has been previously discussed in relation to the loss of motor neurons. Kong and Xu (1998) proposed two distinct scenarios for motor neuron loss: an extended period of gradual motor neuron loss that occurred before the onset of symptoms and another one involving an abrupt loss of motor neurons that corresponded with symptom onset. While this time-frame may be shifted in regards to diminished retrograde transport rates it represents the same biphasic pattern.

When counting the number of ChAT-positive motor neurons the biphasic pattern again emerged. In the G93A mice, there was a plateau in motor neuron numbers from 55 to 115 days. However, while animals at 130 days (artificial end-point) had 44% less motor neurons than age-matched wild-type mice, they only had 32% less motor neurons than at 55 days. The counts of motor neurons in the present study demonstrate a less severe loss than has previously been reported. Although the pattern of motor neuron loss is biphasic, the characteristic loss of motor neurons at the onset of symptoms did not occur. Affected animals at 55 days had 26% less motor neurons than wild-type animals. Although this is different than what has been previously been reported in literature (Chiu et al., 1995), this pattern has been shown in a protracted disease progression G93A mouse model. Feeney and colleagues (2001) reported the initial loss of motor neurons during a presymptomatic stage followed by a period of stabilization and gradual loss coincident

with the onset of symptoms. This gradual loss was observed to extend through to the end-stage of the disease with approximately 50% of motor neurons being lost. There may not be such a pronounced loss of motor neurons at the onset of symptoms as the counts in the 85 day and 100 day groups (closest to the onset of symptoms) have large ranges which could be masking a decrease. Furthermore, when the motor neurons were counted, I did not distinguish between large and small motor neurons, all cells exhibiting ChAT immunoreactivity in the anterior ventral horn were counted. Therefore, I may be including motor neurons that were actively undergoing degeneration while other studies may not have included these cells. The inclusion of all motor neurons could potentially dampen the effect of the selective loss of larger alpha motor neurons as Mohajeri and colleagues (1998) reported that the majority of motor neurons in this area are smaller, gamma motor neurons which remain unaffected until the later stages of disease. This would result in an underestimation of the loss of motor neurons seen as a function of disease progression.

The initial loss of motor neurons could relate to a subset of motor neurons that are particularly vulnerable to injuries mediated by oxidative stress (Feeney et al., 2001). With the initial insult, the loss of some motor units may cause others to begin sprouting. This anatomical plasticity may occur in response to local signals and result in both synaptic and nodal nerve sprouting (Frey et al., 2000) which may account for our observed plateau in cell loss. It has been shown previously that neural-cell adhesion molecule (NCAM) is upregulated in denervated tissue (Sanes et al., 1986; Cunningham, 2005). NCAM may serve as a signal for axonal sprouts to be directed to a particular muscle fiber. The results from our lab demonstrated that NCAM is not significantly

elevated until after the onset of symptoms in the soleus muscle, a predominantly slow-twitch muscle. However, it is known that fast-twitch muscles, such as the medial gastrocnemius, become denervated very early in disease progression (by 47 days of age; Fischer et al., 2004). Therefore, it is possible that there is axonal sprouting occurring during the plateau observed in retrograde transport.

If there was increased axonal sprouting induced by denervation during the progression of symptoms, it would be expected that there would be an increase in the number of cells labelled with Fluoro-Gold. Millecamps and colleagues (2001) demonstrated that increasing the sprouting capabilities of motor neurons by the application of Botulinum Toxin increased the amount of retrogradely transported material, indicating that the toxin increased the efficiency of uptake at the neuromuscular junction due to expanding the axolemma. Additionally, they reported that at symptomatic stages there was a general maintenance of axonal transport that could potentially be attributed to unaffected motor neurons acquiring an increased uptake capacity at the neuromuscular junction presumably through axonal sprouting.

When the number of Fluoro-Gold labelled cells was counted throughout disease progression in this study, there was an interesting result. At 85 days, the number of Fluoro-Gold labelled cells was not significantly different than wild-type controls; however at all other time-points G93A mice had significantly lower numbers of Fluoro-Gold labelled cells. The number of cells labelled with Fluoro-Gold at 85 days was also increased from the previous time-point perhaps indicating increased retrograde transport due to some level of compensatory axonal sprouting. This time-point is coincident with the observed denervation of approximately 60% of the gastrocnemius, extensive atrophy

consistent with persistent denervation (Fischer et al., 2004; Frey et al., 2000), and the observed onset of clinical symptoms. Additionally, 14% of fibres are reported to be intermediately innervated which could represent either active denervation or reinnervation of abandoned neuromuscular junctions by surviving motor units (Fischer et al., 2004). This 85 day time-point would presumably be a period of increased axonal sprouting which could lead to an increased amount of materials being retrogradely transported. However, Frey and colleagues (2001) reported that there was no evidence of expansion of slow motor units at this time-point and fast-twitch fibres are reticent to sprout. The question arises as to how there would be an increase in Fluoro-Gold uptake if there was no axonal sprouting as evidenced by the expansion of motor units. This may indicate that the axolemma is expanding without extensive reinnervation of the muscle fibres due their advanced atrophied state. Consistent with this idea is the finding that axons with no neuromuscular connection are still capable of taking up neurotrophins and other molecules from its surrounding environment. This was shown by implanting a severed axon into a normally innervated muscle, where the motor axon would not be able to form new synapses (Vanden Noven et al., 1993). Therefore, it is conceivable that increased axonal sprouting results in the increased uptake of material without expanding existing motor units. The lack of ability to sprout at the axonal terminal could be one of the factors that conveys increased susceptibility to fast-twitch muscle fibres. Further studies on this G93A strain need to be done in order to assess the amount axonal sprouting and compensatory reinnervation that occurs with disease progression.

To examine whether the decreased percentage of motor neurons labelled with Fluoro-Gold was due to a blockage at the neuromuscular junction, I injected 90 day old

animals and increased the survival period to 72 hours. The 72 hour waiting period was performed based on the observation that the majority of motor neurons were already labelled in the wild-type animals 24 hours after the injection of Fluoro-Gold. After extending the survival period, there was no longer a significant difference in the percentage of ChAT-positive motor neurons labelled with Fluoro-Gold between G93A and wild-type mice. This was contrary to our hypothesis that after 72 hours, more motor neurons will be labelled in the G93A mice but the number will not approximate those seen in wild-type mice. When comparing affected animals 72 hours after injection with a comparable time-point (85 days) 24 hours after injection there was a 20% increase in the percentage of motor neurons labelled with Fluoro-Gold. There was a 10% increase in the percentage labelled cells in wild-type animals. These results indicate that the deficit seen in retrograde transport rates 24 hours after injection is ameliorated if the tracer is given more time to accumulate in the motor neurons. This may occur due to an impairment in the uptake capacity of the motor neuron or a slowing in retrograde transport but there is no evidence of blockage. These results are similar to those reported by Ligon and colleagues (2005). They found that there was no clear difference in neurotracer accumulation between wild-type and G93A mice 72 hours after the injection of Fluoro-Gold.

Comparing the motor neuron numbers

When examining the percentages of motor neurons labelled with Fluoro-Gold from the 72 hour survival period (90 days of age), it seemed that potentially a difference in the number of Fluoro-Gold labelled cells was being masked. However, when the percentages were broken down into the number of ChAT-positive and Fluoro-Gold

positive motor neurons the differences between G93A and wild-type mice were non significant.

When comparing the data from experiment 2 (72 hours after injection, 90 days of age) with experiment 1 (24 hours after injection, 85 days of age), as expected, there was no significant difference in the number of ChAT-positive cells between WT_{72} and WT_{24} or between $G93A_{72}$ and $G93A_{24}$. However, there was no significant difference in the number of Fluoro-Gold positive cells in wild-type animals indicating there was no increase in labelling by extending the survival period. When comparing the $G93A_{24}$ with $G93A_{72}$ the number of Fluoro-Gold labelled cells is significantly increased with the longer survival period. These results are indicative of increased retrograde transport of Fluoro-Gold; however, it is unknown whether this is due to the longer survival period allowing for compensation for slowed uptake at the neuromuscular junction or slowed movement of the retrograde transport machinery.

These results were similar to those obtained by Millecamps and colleagues (2001): 2 days after intramuscular injection of HRP, there were 23% fewer motor neurons labelled; however, there were also 20% fewer Nissl-stained motor neurons. This concurrent decrease suggests that there is a general maintenance of retrograde transport. While this may be the case during mild symptoms such as at 90 days of age, in which there is a plateau in the percentage of motor neurons labelled, as the disease progresses retrograde transport rates are indeed compromised.

Upon review of the 24 hour survival group data, I found that the number of Fluoro-Gold labelled cells was significantly diminished by 55 days of age. Similar results were obtained by Ligon and colleagues (2005) who found that the number of

Fluoro-Gold labelled cells declined by 50 days in the G93A mouse model. While the number of ChAT-positive cells were attenuated at all time-points, there was only a significant difference at 55 and 130 days of age. However, it appears that 55 days of age, the earliest time-point examined, is still a period of maturation and plasticity in the wild-type mice as there is a subsequent increase in weight and a loss of motor neurons observed. The hypothesis of postnatal motor neuron loss is controversial with some researchers showing no loss (Lowry et al., 2001) and others demonstrating motor neuron death during postnatal development (Bennett et al., 1993; Scarisbrick et al., 1990; Crews & Wigston, 1990). My observation of postnatal motor neurons loss is supported by similar trends being observed by Ligon and colleagues (2005) in the same animal model. There are significantly less motor neurons at 55 days in G93A versus wild-type mice. Electrophysiological exams of ALS patients have shown that 80% of motor neurons have already undergone cell death before the first symptoms are detected (Sobue et al., 1983). While the results from my experiments indicate rates of motor neuron death that are not as severe, the death of a significant amount of motor neurons did occur by symptom onset (15%). At end-stage (130 days) the number of motor neurons is approximately 68% of those observed at 55 days and only 50% of the number of wild-type motor neurons at 55 days. This is consistent with results obtained for this mouse model by Chiu and colleagues (1995).

The progression from moderate symptoms to end-stage is very rapid. This acceleration in the loss of motor neurons, skeletal muscle atrophy, and decreased retrograde transport could possibly be compounded by changes in the animal's diet. As the animal loses mobility, their diet is changed from solid to gel form. This is placed on

the cage floor as to allow for easier access but due to severely impaired mobility there is still limited access. Several recent studies have focused on the beneficial effects of adding vitamins and minerals to the diets of G93A mice with conflicting results. There have been marked abnormalities in carbohydrate metabolism observed in ALS patients and animal models with the end result being an imbalance between energy intake and energy expenditure. Consistent with the hypothesis of a diet related disease acceleration, a study by Gonzalez de Aguilar and colleagues (2005) found that feeding transgenic mice a high-fat diet inhibited denervation, prevented the loss of large motor neurons and extended life span by 20%. The hastened disease progression observed in the animals in the later stages of the disease may in part be due to the inadequate intake of calories due to a restricted diet.

Defects in the axon: uptake or transport?

Axonal growth and maintenance involves a variety of mechanisms that include microtubule assembly, the transport of growth factors from the target to the cell body, and communication regarding the activity levels of the target (Jablonka et al., 2003). Any defects in these mechanisms could play a role in the development of neuromuscular diseases; it has been shown that disruption of retrograde transport in vitro and in vivo initiates the degeneration of motor neurons. Animal models of ALS have been created using various mutations in the genes that encode for dynein, dynactin, and neurofilaments which are key components in retrograde transport (LaMonte et al., 2002; Collard et al., 1995; Ligon et al., 2005; Ligon et al., 2004; Puls et al., 2003; Hafezparast et al., 2003; Kieran et al., 2005). Furthermore, the aggregation of SOD1 has been shown to disrupt the transport capabilities of dynein and lead to the accumulation of neurofilaments

(Bruijn et al., 1998; Williamson et al., 1998; Kieran et al., 2005). These results indicate that defects in retrograde transport are sufficient to cause degeneration. However, the question remains as to where the deficit originates: is there a problem with the transport machinery or the neuromuscular junction?

While it has been shown that mutating the retrograde transport machinery can result in neurodegeneration, the state of the machinery in other models of ALS has not been well characterized. In a study structured similar to ours, Ligon and colleagues (2005) injected G93A mice with Fluorogold at various time-points and observed retrograde transport. They reported that there was diminished retrograde transport by 50 days. In accordance with the results of the present study, they found that increasing the survival period to 72 hours abolished any difference due to genotype. Additionally, they reported that a decrease in muscle strength, as assessed by grip tests, correlated temporally with attenuation in Fluoro-Gold uptake. Using immunohistochemical analysis, they found no significant change in the expression levels of dynein or dynactin subunits in the G93A spinal cord. However, using primary motor neuron cultures they found that the presence of mutated SOD1 (G85R) caused a disruption of dynein and resulted in the formation of large aggregates of dynein and SOD1. These results correspond with the present study demonstrating that alterations in retrograde transport rates are an early event. However, they were also unable to clarify whether deficits in the neurotracer uptake or the transport itself caused the degeneration.

At the end-stage of the disease there are clearly signs that the retrograde transport machinery has been disrupted (Ligon et al., 2005; Williamson & Cleveland, 1999). It has been hypothesized that initially, reduced retrograde transport may be due to a reduced

amount of materials available to be transported. Initial arguments for the theory of diminished uptake capacity came from the wobbler mouse (Mitsumoto et al., 1990). In this model, the affected cervical motor neurons had decreased HRP labelling, but the less affected lumbar motor neurons had increased labelling (Mitsumoto et al., 1990). Retrograde transport rates were normal in lumbar motor neurons but decreased in the cervical cells. This increase in retrogradely transported materials with normal rates could be accounted for by sprouting of the lumbar motor neuron axon terminals. While the forelimb muscles displayed a significant degree of atrophy, there was no denervation-induced atrophy observed in the hind limbs. As the amount of retrogradely transported material depends on membrane turnover at the neuromuscular junction (Mitsumoto et al., 1990) any axonal sprouting should increase the amount of materials transported. However, even sprouting has its limitations. In the wobbler mouse, by 3 months only 30% of cervical motor neurons remain (Haenggeli & Kato, 2002) and there is aggressive sprouting of the remaining axons in an attempt to reinnervate the denervated fibers (Mitsumoto et al., 1990). However, this aggressive sprouting may be decreasing the uptake capacity of the neuron by rapidly expanding the axolemma in a last-ditch effort to reinnervate abandoned muscle fibers.

I hypothesized that there would be a small increase in the percentage of motor neurons labelled with Fluoro-Gold at 120 days of age due to the compensatory reinnervation of abandoned neuromuscular junction as postulated by Fischer and colleagues (2004). However, there was no such increase which may be accounted for by the return of any endocytosed vesicles to the plasma membrane in order to expand the aggressively sprouting axolemma (Mitsumoto et al., 1990). At this point in the disease,

retrograde transport may further be attenuated by the lack of transport machinery available as anterograde transport is diminished, resulting in the reduced delivery of dynein and its regulators (Williamson & Cleveland, 1998). This may explain the severe drop in the number of Fluoro-Gold labelled cells and the diminished percentage of motor neurons labelled with Fluoro-Gold observed from 115 to 130 days. Results from the present study indicate that decreases in retrograde transport occur at an earlier age that what has been reported for alterations in anterograde transport in this animal model. The subsequent decreases in anterograde transport may be due to a form of negative feedback. Impairment in the uptake capacity of axon terminals could lead to the degeneration of the motor neuron. Retrograde transport provides essential information regarding the innervation status and the environment of the neuromuscular structure. If there is a lack of communication from a target to the motor neuron this may be perceived as a decrease in activity and a corresponding decrease in the amount of materials transported to that neuromuscular junction could occur. I hypothesize that reduced retrograde transport signals to the motor neuron cell body that the same level of support is no longer required at the neuromuscular junction. The cell body would adjust to the perceived diminished activity by decreasing the amount of trophic support and supply of key components to the neuromuscular junction. The diminished support may then exacerbate any problems already existing within the distal axon resulting in a perpetuating negative feedback cycle.

In this study, the number of Fluorogold labelled cells was significantly attenuated by 55 days of age, and Ligon and colleagues (2005) showed a deficit as early as 50 days. This deficit may even precede denervation in this animal model. Fischer and colleagues

(2004) reported that at 28 days of age there was 100% innervation of the gastrocnemius but by 47 days there was 40% denervation. Together, this indicates that the uptake capacity of selected motor neurons is compromised resulting in the denervation of the muscle. This idea is further supported by our observation that after 72 hours there are more motor neurons labelled with Fluoro-Gold. The increase in survival time may allow for a slower uptake system to compensate. While compensation with Fluoro-Gold may occur due to its persistence at the neuromuscular junction, limited diffusion capabilities and long half-life (Schmued & Fallon, 1986) many molecules such as growth-factors, have shorter half-lives and may be degraded within the synaptic cleft if not taken up by the neuromuscular junction in a timely manner. In the developing nervous system, there is competition to innervate muscle fibers (Glover, 2000). If a motor neuron does not receive adequate amounts of growth factors and key nutrients from the target it removes its axon terminals and degenerates. Although it has been shown that muscle phenotype is established around 30 days (Frey et al., 2000) it is possible there may be some motor neurons that are in the process of removing their axon terminals and have not began to degenerate as motor neurons have been shown to survive for extended periods without having functional neuromuscular junctions (Vanden Noven et al., 1993).

It is possible that the uptake mechanism itself is unchanged with disease progression. Conversely, the decreases in retrograde transport may be due to a decreased number of axon terminals available to take up the tracer. Sagot and colleagues (1998) demonstrated that the administration of neurotrophic factors to wild-type mice did not affect the speed of retrograde labelling of motor neurons. The rate of transport may be operating an optimal level. This can be demonstrated by the fact that although there was

an increase in the percentage of Fluoro-Gold labelled cells in wild-type mice at the 72 versus the 24 hour survival period, the increase was smaller than that seen in G93A mice (10% vs. 20% respectively). This can be explained by neurons exhibiting a basic rate of membrane turnover. If the rate of turnover is not changing, as would be the case unless there was aggressive axonal sprouting taking place, then the retrograde transport rate should not be expected to change.

There is no clear indication of whether the deficit in retrograde transport is the result of an impairment in the uptake capacity of the neuromuscular junction or of some problem with the retrograde transport machinery and the axon itself. In the pmn mouse, the application of a tracer to the cut sciatic nerve showed that labelling after 24 hours was half that of wild-type mice (Sagot et al., 1998) which would indicate that there was a deficit in the axon and perhaps the retrograde transport machinery. However, in the same paper it was reported that after intramuscular injection, pmn mice were slower to show motor neuron cell body labelling. It is possible that there is an initial deficit in one system that creates a subsequent deficit in the other within a small temporal frame that has yet to be observed. It appears that some problem at the neuromuscular junction results in the decreased retrograde transport of key nutrients leading to an attenuation in anterograde transport that results in the denervation and subsequent atrophy of skeletal muscle fibers ultimately ending in the degeneration of the motor neuron cell body. The degeneration of motor neurons in later stages of disease progression may be hastened by the observation that there is a loss of synaptophysin immunoreactivity on lumbar motor neurons temporally coincident with the onset of symptoms (Zang et al., 2005). This

would result in the loss of communication between lower motor neurons in the spinal cord and upper neurons in the cortex and brainstem.

There are still many questions to be answered regarding retrograde transport and the mechanisms involved are just starting to be revealed. Recently, it has been hypothesized that there may be different uptake mechanisms that have selective vulnerability. This has been demonstrated in novel experiments using atoxic fragments of tetanus and botulinum toxins (Deinhardt & Schiavo, 2005). Additionally, some results based on longer survival periods may not mirror endogenous activity as Deinhardt and Schiavo (2005) have shown that the saturation of one uptake mechanism can result in the recruitment of another, a situation that may not happen *in situ*. The mechanism of vesicle sorting within the axon terminal in regards to how it is decided that certain materials are retrogradely transported has also yet to be elucidated. It is possible that while uptake mechanisms remain intact, the sorting mechanism is unable to distinguish vesicles bound for the cell body resulting in those materials not being retrogradely transported. Further studies need to be done to establish this sorting mechanism.

Implications for gene therapy

Currently there is no cure for ALS and treatments thus far have aimed to limit muscular atrophy and improve patient quality of life. Recently, gene therapies involving the viral delivery of neurotrophic substances through intramuscular injection have shown to be efficacious in animal models. The majority of research has focused on treating animals that were presymptomatic or just starting to show symptoms. While these experiments have shown improvements in lifespan (Kaspar et al., 2003; Azzouz et al., 2004) these treatments were at time-points that would not be possible in ALS patients.

The majority of ALS patients are not diagnosed until after symptom onset, a time at which close to 32% of motor neurons may already be lost (Swash et al., 1986), the majority of the muscle fibers of the distal limbs are undergoing denervation, there is significant muscular atrophy, and retrograde transport is significantly impaired.

Regardless of whether the defect is in the uptake capacity of the axon terminal or within the retrograde transport machinery itself, an attenuation in retrograde transport occurring with disease progression will affect many proposed gene therapies. Experiments need to be done involving the viral delivery of trophic factors at later stages in disease progression in order to evaluate the validity of these strategies.

Future studies

In order to clarify whether the initial defects occurs at the neuromuscular junction or in the retrograde transport machinery, further studies must be done. By transecting the sciatic nerve at both a distal and proximal region in relation to the spinal cord, researchers will be able to detect any changes in rate within these areas. Differences may indicate a problem with the retrograde transport machinery. Alternatively, by inducing terminal axonal sprouting in an ALS mouse model through the administration of Botulinum Toxin or GAP43 at various time-points throughout disease progression, researchers would be able to clarify whether sprouting has an effect on retrograde transport in a compromised system. Increased axonal sprouting should lead to an increased uptake of materials at the neuromuscular junction, as demonstrated by Millecamps and colleagues (2001). Once sprouting is induced, if retrograde labelling is not increased then it is possible that there is a defect in the retrograde transport machinery or within the sorting mechanism in the axon terminal.

2.7 Conclusion

The results from this study demonstrate that deficits in retrograde transport occur relatively early in disease progression in the G93A mouse model of ALS preceding observed deficits in anterograde transport, the onset of clinical symptoms, the loss of motor neurons and coinciding with the denervation of fast-twitch muscles. These results suggest an impairment in the distal axon involving the uptake mechanisms at the neuromuscular junction, the sorting of vesicles for retrograde transport, or the retrograde transport machinery itself. It was found that increasing the survival time abolished transport rate defects leading to the postulation that there may be slowed uptake of materials at the neuromuscular junction but that uptake is not blocked. The differential changes in retrograde transport throughout disease progression, specifically the plateau from 70 to 115 days, may be due to compensatory axonal sprouting in response to denervation. This phenomenon appears to begin before the onset of symptoms and is overcome shortly thereafter consistent with the overburdening of surviving motor units.

While this study characterized retrograde transport as a function of disease progression and of symptomatology, it did not clarify whether the initial defect lies in the neuromuscular junction or within the retrograde transport machinery. I speculate that the initial defect lies in the ability of the neuromuscular junction to take up key nutrients and therefore signals to the motor neuron cell body that the target does not require the same level of support leading to a pathological cascade the terminates in the denervation of the muscle fiber and the subsequent degeneration of the motor neuron. Further studies must be done in order to clarify the pathological mechanisms involved in the attenuation of retrograde transport and the order in which they occur.

TABLES AND FIGURES

Table 1 Number of ChAT-positive and Fluoro-Gold-positive motor neurons. All values reported as mean ± standard deviation.

Genotype	Age (in days)	# ChAT +ve MN Counted	# FG +ve MN Counted	N
Wild-type	55	100 ± 12	86 ± 10	5
G93A	55	74 ± 16*	61 ± 13*	5
Wild-type	70	73 ± 7	61 ± 5	5
G93A	70	61 ± 8	39 ± 4*	5
Wild-type	85	79 ± 9	60 ± 10	4
G93A	85	70 ± 16	43 ± 14	4
Wild-type	100	70 ± 16	57 ± 12	5
G93A	100	59 ± 20	34 ± 15*	5
Wild-type	115	80 ± 13	68 ± 12	5
G93A	115	66 ± 8	33 ± 5*	5
Wild-type	130	77 ± 18	67 ± 17	7
G93A	130	51 ± 12*	8 ± 8*	6

G93A (affected) vs. wild-type (control) mice. The number of motor neurons reported reflects the number counted from 8 sections per animal. There was a significant effect of time progression on the number of ChAT-positive and Fluoro-Gold-positive motor neurons counted ($p<0.001$). This symbol (*) indicates significant difference from Wild-type ($p<0.05$).

Table 2 **Percent of motor neurons (MN) displaying Fluoro-Gold (FG) staining as a function of disease progression. All values reported as mean ± standard deviation.**

Symptom Group	Mean Age	Age Range	% of MN displaying FG	N
Wild-type	95 ± 5	55 – 130	84 ± 6	31
G93A – None	65 ± 3	55 – 85	72 ± 12	11
G93A – Mild	93 ± 3	85 – 100	59 ± 8	6
G93A – Moderate	115 ± 5	100 – 130	49 ± 15	5
G93A – Severe	123 ± 4	100 – 130	26 ± 24	8

Comparison based on the symptomatology on day of euthanasia. There was a significant difference between all symptom groups and wild-type controls ($p<0.001$). There was also a general decrease throughout disease progression ($p<0.001$).

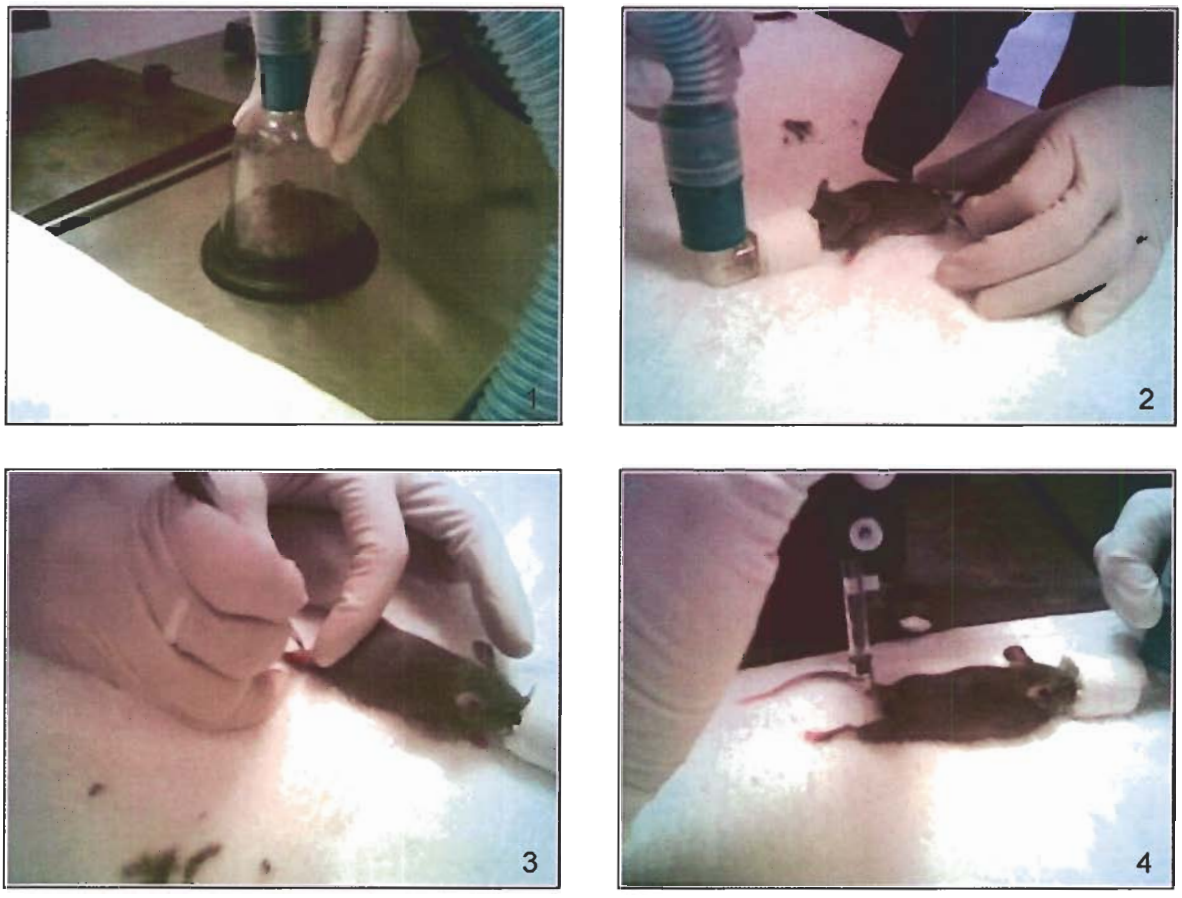

Figure 1 Fluoro-Gold injection procedure.

Animals were anesthetized in an induction chamber with 5% Isoflurane. Animals were then placed on a respirator with a 2.5% isoflurane flow rate. The right calf area was shaved and a 1mm incision above the belly of the gastrocnemius was made with a scalpel. 5µl of 4% Fluoro-Gold was then injected directly into the superficial medial gastrocnemius over a 3 minute time period with a Hamilton syringe controlled by a micromanipulator. After the injection the 33-gauge needle was left in the muscle for 1 minute to prevent the uptake of any Fluoro-Gold via capillary action. Polysporin was applied to the incision and the animals recovered under heating lamps for 30 minutes before being returned to their cages.

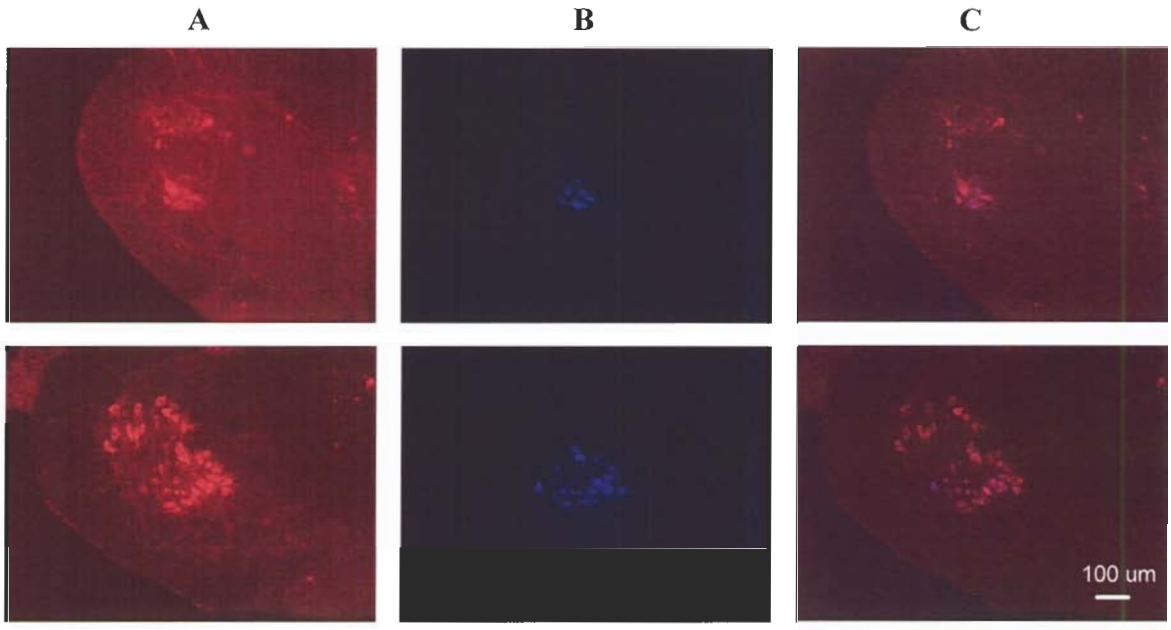

Figure 2 Labelling of motor neurons in control mice at two segmental levels.

Motor neurons innervating the medial gastrocnemius were consistently observed in the dorsolateral aspect of the anterior ventral horn. (A) ChAT staining of motor neurons in the anterior ventral horn. (B) Fluoro-Gold staining in the anterior ventral horn. (C) Overlay of ChAT and Fluoro-Gold in the anterior ventral horn. 10X Magnification.

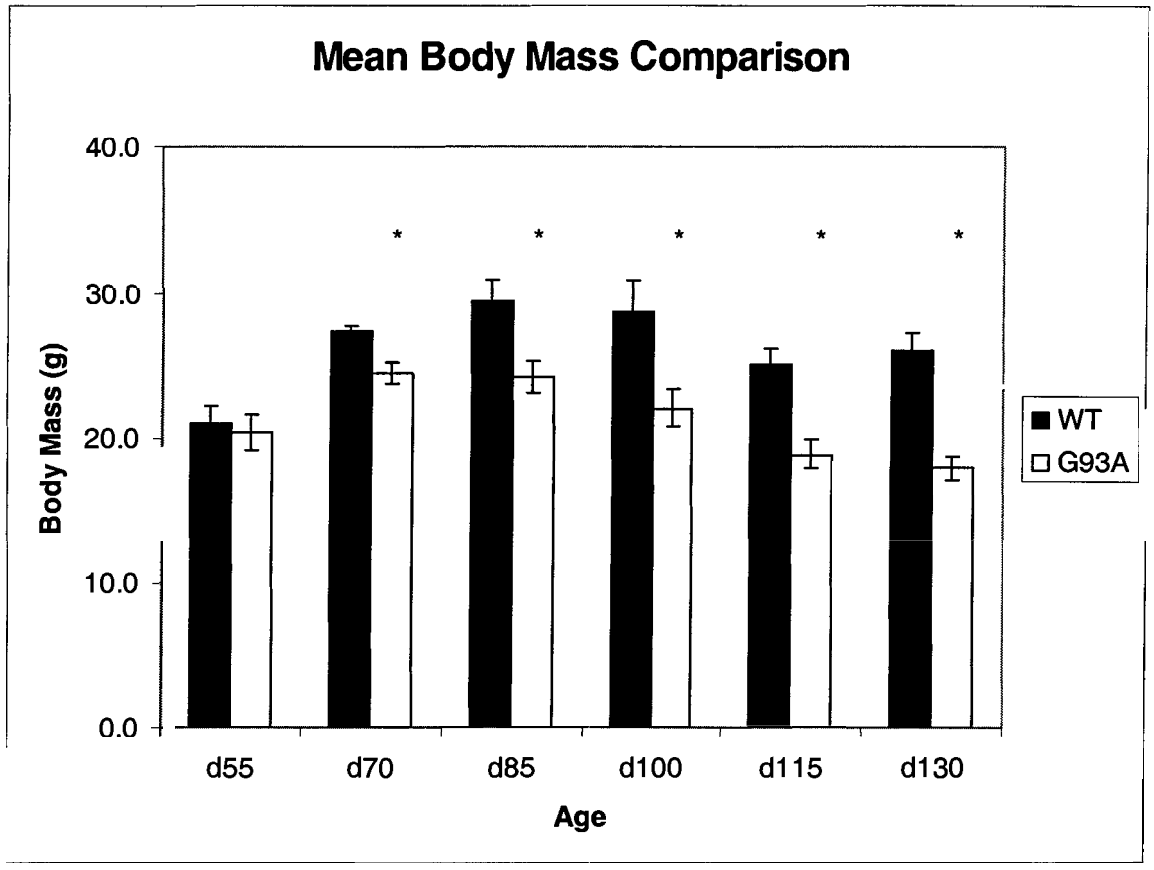

Figure 3 **Mean body mass comparison. All values reported as mean body mass ± standard error.**

G93A (affected) vs. wild-type (control) mice. This symbol (*) indicates a significant difference from Wild-type ($p<0.03$).

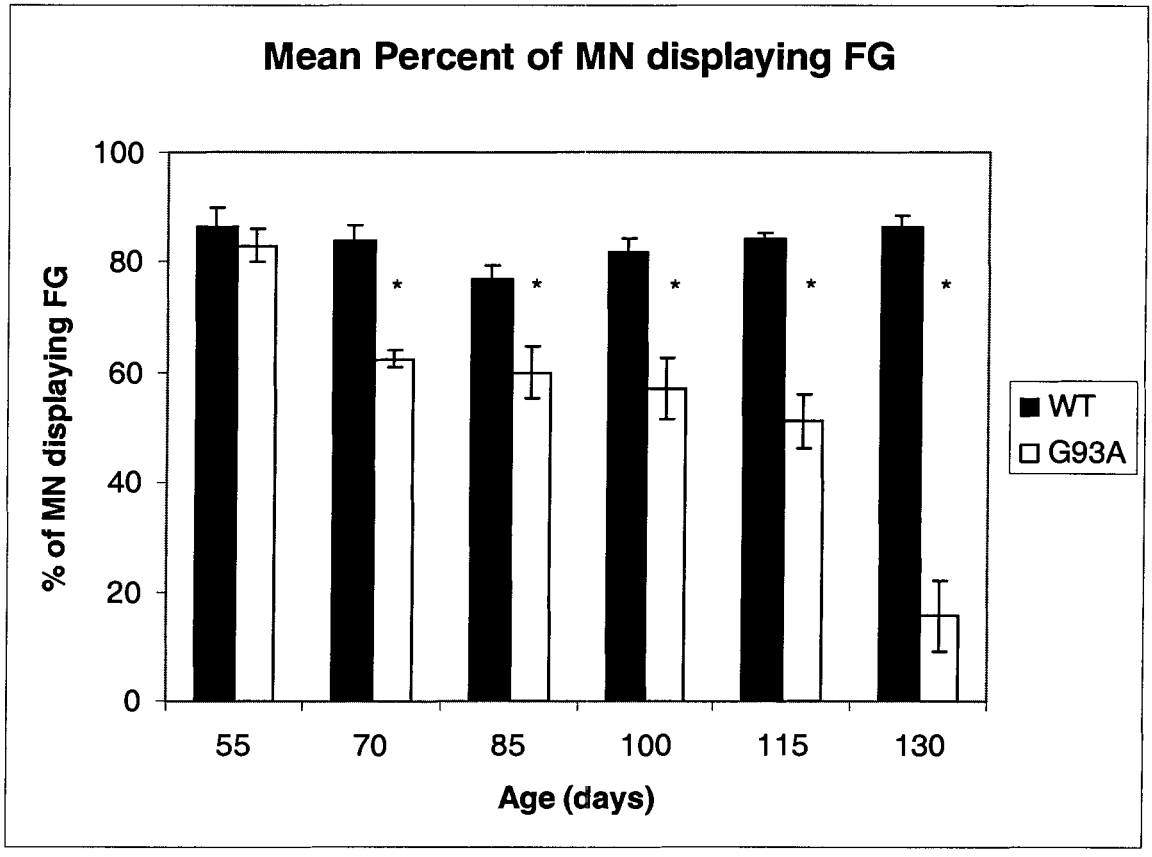

Figure 4 Mean percentage of motor neurons displaying Fluoro-Gold as a function of disease progression. All values are reported as mean ± standard error.

G93A (affected) vs. wild-type (control) mice. This symbol (*) indicates a significant difference from Wild-type controls ($p<0.03$). There is a general decline in the percentage of motor neurons displaying Fluoro-Gold over time.

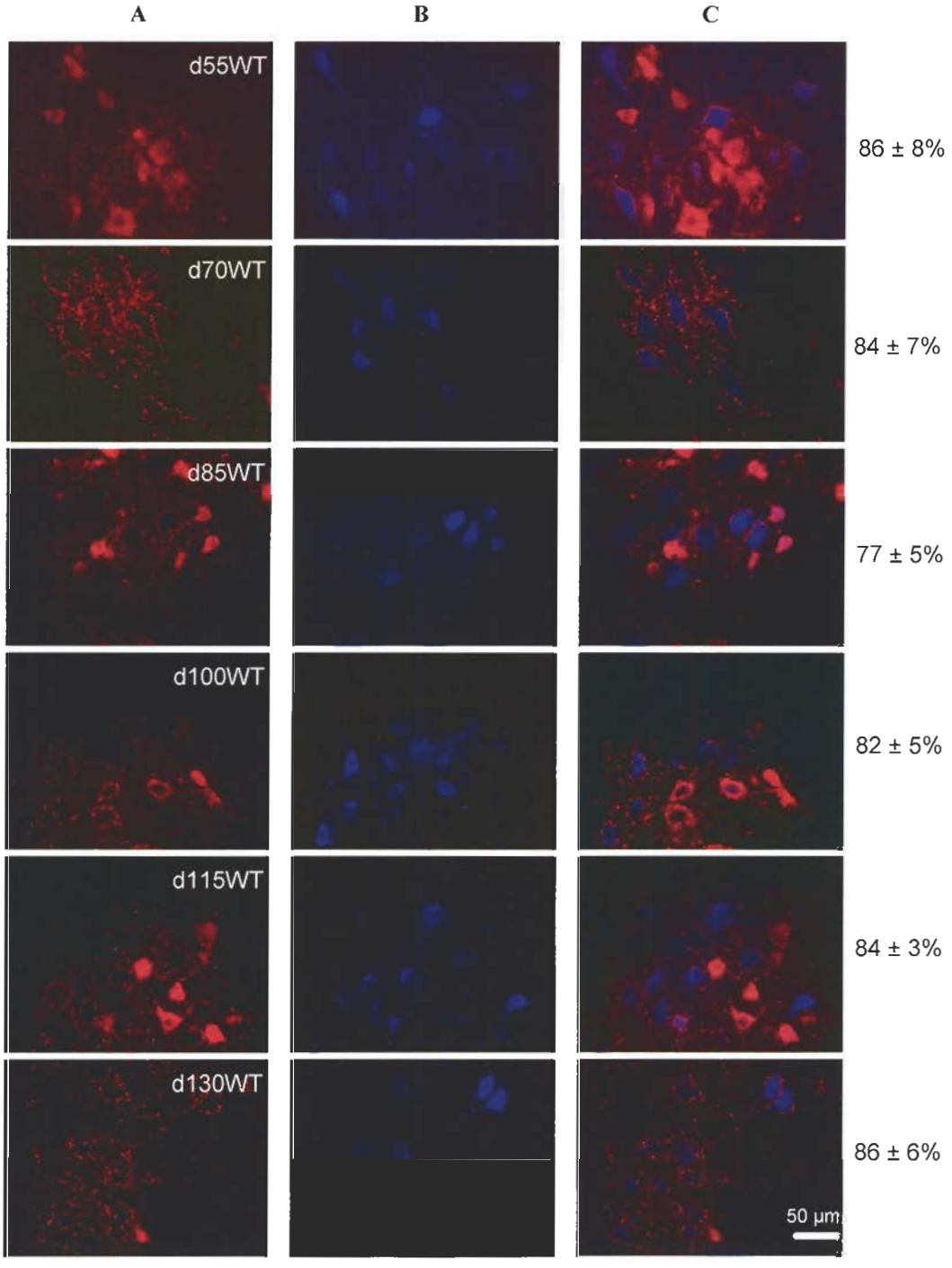

Figure 5 ChAT-immunolabelled lumbar spinal cord: wild-type.

Sections were immunolabelled for ChAT, a marker of the motor neuron cell body (Column A), and examined for Fluoro-Gold (Column B). Image overlay (Column C) allows for the visualization of the number of ChAT-positive motor neurons displaying Fluoro-Gold which is a relative index of retrograde transport rate. Wild-type animals across time-points have 80% of ChAT-positive motor neurons displaying Fluoro-Gold. 40X Magnification.

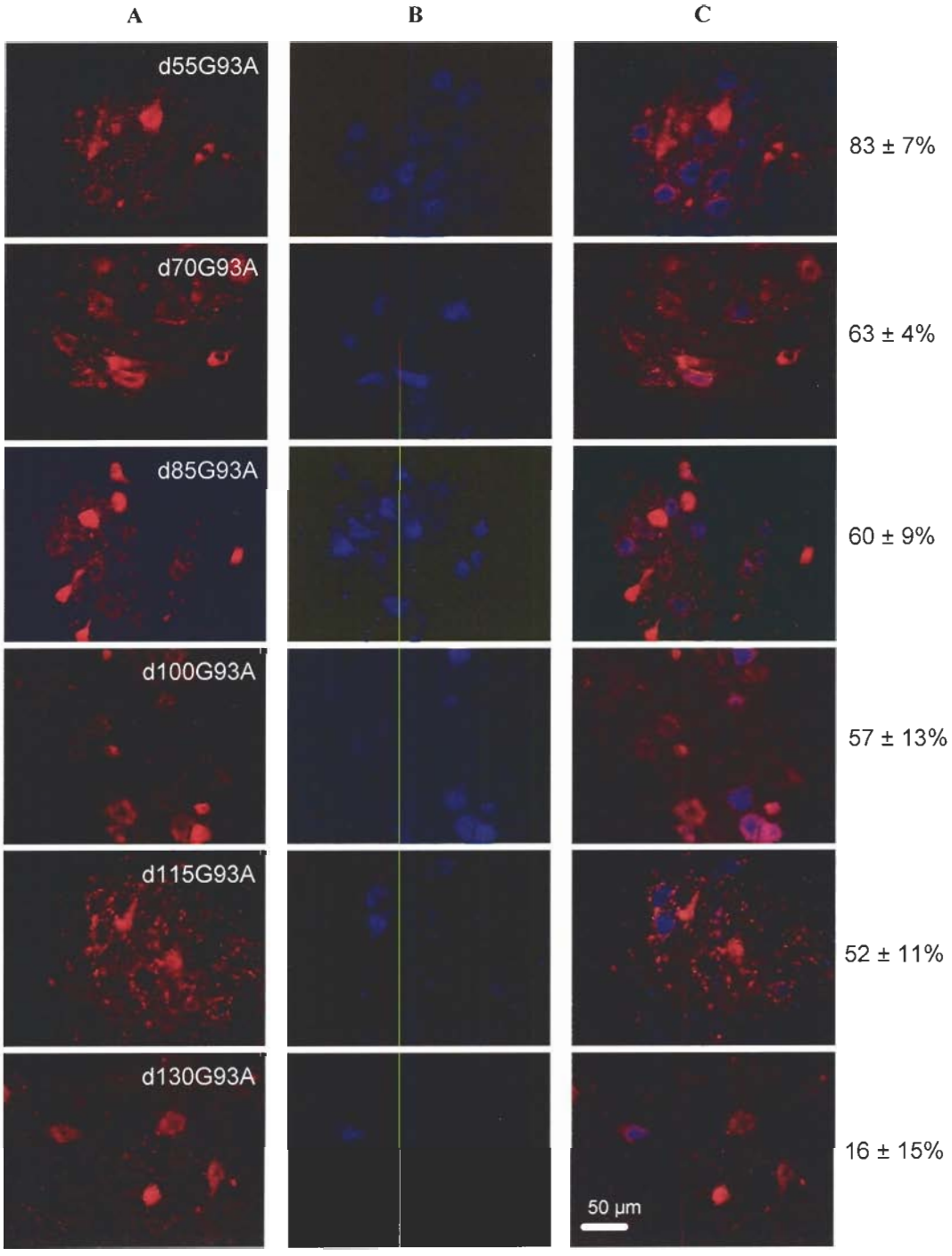

Figure 6 ChAT-immunolabelled lumbar spinal cord: G93A.

Sections were immunolabelled for ChAT (Column A), and examined for Fluoro-Gold (Column B). Image overlay (Column C) allows for the visualization of the number of ChAT-positive motor neurons displaying Fluoro-Gold. There is a significant decline in the number of ChAT-positive motor neuron displaying Fluoro-Gold across time-points. 40X Magnification.

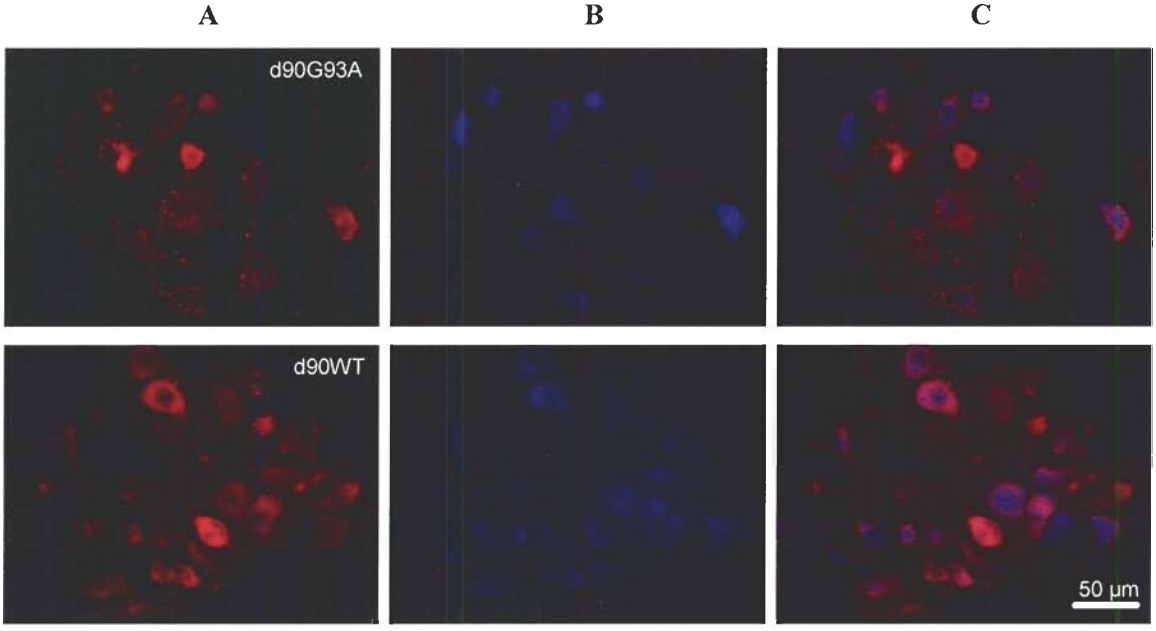

Figure 7 ChAT-immunolabelled lumbar spinal cord: G93A vs. wild-type.

Sections were immunolabelled for ChAT, a marker of the motor neuron cell body (Column A), and examined for Fluoro-Gold (Column B). Image overlay (Column C) allows for the visualization of the number of ChAT-positive motor neurons displaying Fluoro-Gold which is a relative index of retrograde transport rate. At day 90 there was no significant difference between groups: G93A mice had 80 ± 12% of ChAT-positive motor neurons displaying Fluoro-Gold, wild-type mice had 87 ± 4%. 40X Magnification.

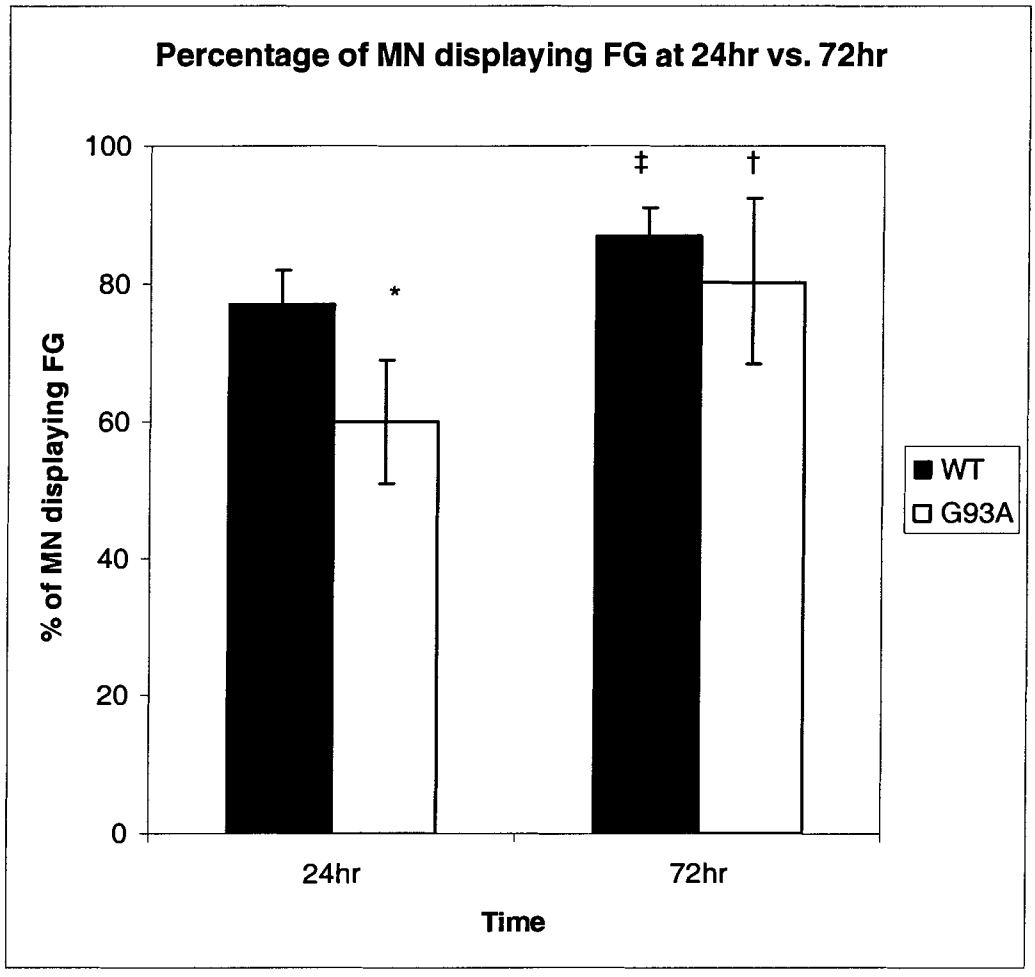

Figure 8 **Percentage of motor neurons displaying Fluoro-Gold at 24 and 72 hours. All values reported as mean ± standard error.**

Comparison of the percentage of motor neurons displaying Fluoro-Gold 24 hours after injection (85 days old) and 72 hours after injection (90 days old). This symbol (*) indicates G93A mice had a significantly lower percentage of motor neurons displaying Fluoro-Gold than wild-type mice ($p<0.01$). After 72 hours, there was no significant difference between 90 day old G93A mice and wild-type mice. This symbol (†) indicates that after 72 hours G93A mice had a significantly greater percentage of motor neurons displaying Fluoro-Gold than G93A mice after 24 hours ($p<0.02$). This symbol (‡) indicates that after 72 hours wild-type mice had a significantly greater percentage of motor neurons displaying Fluoro-Gold than wild-type mice after 24 hours ($p<0.02$).

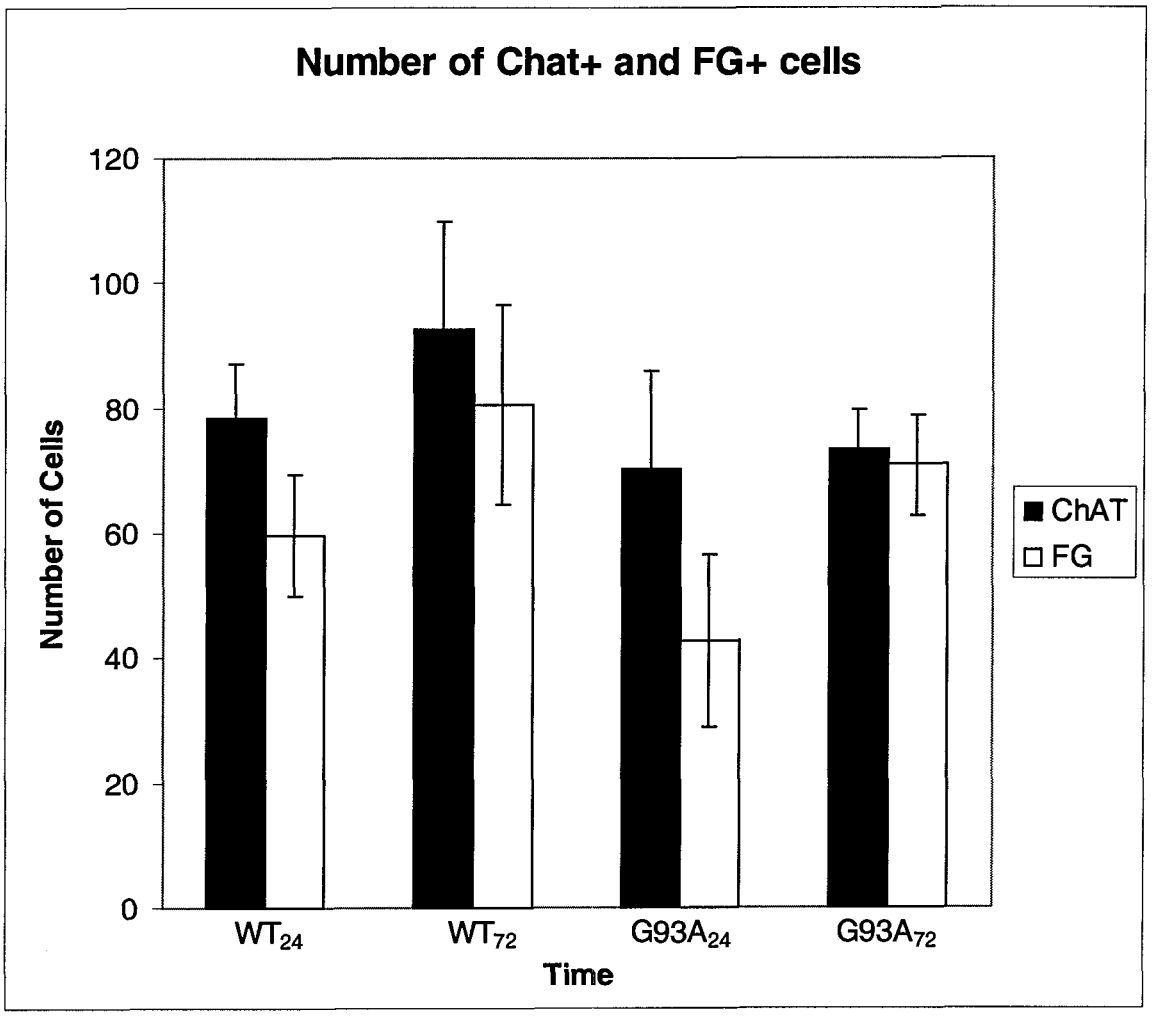

Figure 9 **Number of ChAT-positive and Fluoro-Gold-positive cells at 24 and 72 hours. All values reported as mean ± standard error.**

Comparison of the number of ChAT-positive and Fluoro-Gold-positive cells in both wild-type and G93A mice 24 hours after injection (85 days old) and 72 hours after injection (90 days old). This symbol indicates (*) significant difference in the number of Fluoro-Gold-positive $G93A_{24}$ vs. $G93A_{72}$ ($p<0.03$). There is no significant difference in ChAT-positive cells across time in both G93A ($G93A_{24}$ vs. $G93A_{72}$) and wild-type mice (WT_{24} vs. $WT_{72.}$). There is no significant difference in Fluoro-Gold-positive cells between WT_{24} vs. $WT_{72.}$

APPENDICES

Appendix A: Genotyping Protocol[2]

DNA Isolation

Solutions

1X Tris-EDTA (TE) Buffer (pH 8.0)

10mM	Tris-Cl (Trizma Base)	MW 121.1
1mM	EDTA (ethylene diamine tetra acetic acid)	MW 336.2

Low TE Buffer (0.1X TE, pH 7.6)

5ml	1X TE
45ml	ddH_20

Chelex (Fluka, product #95577 100-200 mesh)

5% w/v in low TE

Proteinase K (Sigma-Aldrich, product # P-2308)

20mg/ml in ddH_20

RNase buffer

10mM	Tris-Cl (pH 7.5)	MW 121.1
15mM	NaCl	MW 58.5

RNase A (Sigma-Aldrich, product # R-4876)

10mg/ml in Rnase buffer
Boil for 15 minutes

Chelex Solution (300ml – enough for two samples)

250µl	Chelex	5%w/v
25µl	Proteinase K	20µg/µl
25µl	RNase A	10µg/µl

Protocol

** All steps are to be performed using autoclaved pipette tips and eppendorf tubes **

[2] (adapted from Hu et al., 2003)

1. Add 150µl Chelex solution to ear punch sample. When collected sample, ensure that the forceps are adequately cleaned with 70% ethanol and then sufficiently rinsed with sterile saline as failure to do so may result in DNA fragmentation.
2. Vortex sample and chelex solution and ensure sample is within solution. Place in 55°C[3] water bath for 30 minutes (vortex once at 15 minutes during incubation).
3. Vortex and ensure sample is within solution then place tube in heating block at 100°C for 8 minutes.
4. Centrifuge for 15 minutes at 12 000 rpm
5. Remove supernatant (be careful not to disrupt beads) to clean, autoclaved eppendorf tube and use as DNA template IMMEDIATELY (* if not freeze DNA template)

PCR Reaction

Solutions

PCR Mixture

Template	1µl
Primer mSOD1[4]	0.5µl
Primer mSOD2[5]	0.5µl
10X Buffer	2.5µl
dNTPS[6]	2.5µl
$MgCl_2$	0.5µl
DdH_20	17.2µl
Taq[7]	0.3µl
	25.0µl

PCR Setting

95°C	5	min	
94°C	30	sec	30 cycles
56°C	30	sec	
72°C	30	sec	
94°C	30	sec	1 cycle
56°C	30	sec	
72°C	10	sec	
4°C	∞		

[3] Ensure that temperatures are exact as failure to do so may result in the degradation of DNA sample.
[4] 5' to 3': CAT CAG CCC TAA TCC ATC TGA; desalted; 50nmole; Invitrogen
[5] 5' to 3': CGC GAC TAA CAA TCA AAG TGA; desalted; 50nmole; Invitrogen
[6] 100mM stock: 10µl dCTP, 10µl dTTP, 10µl dATP, 10µl dGTP, 460µl ddH_20; Amersham
[3] Add Taq polymerase last

Protocol

1. Determine the number of samples being run and multiply the components of the PCR by that number + 1. Combine the reagents (excluding the DNA samples) in an autoclaved eppendorf tube and mix sufficiently. Aliquot the PCR mixture into autoclaved PCR tubes.
2. Add the DNA samples to each individual PCR tube, ensuring to use a new pipette tip for each sample to avoid contamination.
3. Gently mix the PCR mixture with the DNA sample by flicking the bottom of the PCR tube. Ensure there are no air bubbles in the solution.
4. Place the tubes in the wells of the PCR machine and close the lid.
5. Select the appropriate cycle as detailed above.
6. Once the PCR reaction is complete (approximately 2 hours) then remove PCR tubes and proceed to the gel electrophoresis step. Samples may be stored at -20°C but are best used fresh.

Gel Electrophoresis

Solutions

Agarose Gel (1% w/v)

2g	Agarose
200ml	0.5X Tris- Acetate EDTA (TAE buffer)
20µl	Ethidium Bromide

Heat agarose and buffer until solution is clear (on a magnetic stir plate). Add Ethidium Bromide before pouring gel solution into tray forms.

50X Tris-Acetate-EDTA (TAE buffer)

242g	Tris Base
57.1ml	Acetic Acid
100ml	0.5M EDTA

Add ddH_2O to 1L. Adjust pH to 8.5. Dilute with ddH_2O to appropriate working concentrations.

Protocol

1. Add 10µl of PCR template to 1-2 µl of loading dye and mix sufficiently on a strip of parafilm.
2. Place gel in the Mupid 21 electrophoresis apparatus with the black stripe facing right.

3. Ensure that 0.5X TAE buffer is completely covering gel and has infiltrated the wells.
4. Load gel lanes carefully with 8-10µl of sample using autoclaved tips (do not pierce the gel).
5. Cover the system firmly with appropriate lid and plug in the power source.
6. Run at 100V for approximately 25-40 minutes.
7. Once gel is finished, remove from apparatus and wrap in plastic.
8. Visualise under UV light – animals that are affected will have a band fluoresce at 236 base pairs, animals that are not affected will not have this band.

Appendix B: Disease Progression Characteristics

Normal Mouse - the hind legs are extended and splay upon lifting

Very early signs - the legs are no longer splayed upon lifting- usually reported as questionable

Early signs

- start to see flexion in one or both of the hind legs
- see progression in flexion from slightly flexed to very flexed
- start to see muscle atrophy, evident in the hips and hind legs at first, usually at point of moderate degree of flexion
- rolling gait (whole body moves with each step; progresses from slight to pronounced)or paddling gait - with or without the hind feet being cow-hocked (toes pointed out)
- they have a hunched posture (from slight to very hunched)
- see a progression in muscle atrophy on hips and up onto the back of the mouse.

Moderate Signs

- hind foot knuckling - they start to drag toes (on one or both hind feet) but still able to correct it at first until they reach point of constant knuckling- not able to lift foot up to correct
- they may become less active in this stage.
- males develop a rough coat- females normally don't

Advanced Stages

- atrophy in the back in when the mouse has lost its hunched posture they have reached maximum flexion in the hind limbs
- some of the males have urine staining

- display partial to complete paralysis of one or both of the hind legs
- weakness can then progress up into the front legs so that they are walking with their body very low to the ground
- Once roll over starts then we count how long they are in lateral recumbency. **Endpoint is lateral recumbency of 10 seconds.**

Disease Progression Criteria provided by Mary Dearden, Animal Care Facility, SFU

Appendix C: Immunohistochemical Staining Protocol

OCT Mounting

1. Place dry ice on metal working surface until it is sufficiently cold.
2. Apply Optimal Cutting Temperature Medium (OCT) to metal surface in the shape of a circle, it should be approximately the size of a quarter. This will serve as the base of the mold. It is necessary to keep the mold surrounded by the dry ice.
3. Once almost set (OCT should be slight tacky in the middle of the circle) gently set the caudal tip of the spinal cord into the OCT. This should be done with atraumatic forceps taking great care not to squish the spinal cord.
4. Once the OCT has set and spinal cord stays in place, apply OCT around the spinal cord a small amount at a time in order to build up the mold in a pyramidal manner.
5. Once this application has set, apply again until the spinal cord is sufficiently covered.
6. Gently remove mold from metal working surface, wrap in parafilm and tin foil then store at -80°C until ready to use.

Cryosectioning

1. The cryostat should be set at approximately 15-17°C. Sections will be cut at 30μm.
2. Before starting, wipe down all surfaces with a small amount of ethanol. Check the sharpness of the blade, if dull replace with new Feather microtome blade).
3. To secure sample to the stage, apply a small amount of OCT to the stage and then press sample onto it. Allow OCT to sufficiently set before attempting to cut.
4. Place stage into stage holder and align properly with blade. Secure stage and recheck alignment of sample.
5. Before slicing sections: set up a 4 X 6 well tissue culture plate filled 1XPBS that you can place sections into.
6. Turn off safety on the cryostat handle and begin slicing. Each spinal cord section should be picked up with the paintbrush and gently placed into the 1XPBS in the appropriate well.
7. Sections are able to be stored in the 1X PBS solution for up to 48 hours at 4°C. For samples not being used within that timeframe, sections can be placed in de Olomos solution[8] at stored in eppendorf tubes at -20°C until needed.

[8] De Olomos solution (500ml): 5g PVP-40, 150g sucrose, 150ml Ethylene Glycol, 25ml 20X PBS. Top up to 500ml with ddH_2O. On low heat, stir until dissolved. Store at -20°C.

Immunohistochemical Staining

Solutions

20X Phosphate Buffered Saline (Stock Solution, 100ml)

1. Make up the following solution in about 90 ml (use a 100 ml beaker):
   - 129mM (0.129 M) Sodium Phosphate Dibasic Anhydrous (MW 142) or Dihydrate (MW 178)
   - 29.4mM (0.0294 M) Potassium Phosphate Monobasic (MW is usually 136.1)
   - 2.74mM Sodium Chloride (MW 58.45)
   - 54mM Potassium Chloride (MW 74.55)
2. Place on an electromagnetic stirrer, and heat with stirring to dissolve.
3. Once all the salts have dissolved feel the outside of the beaker. If hot cool the solution to room temperature by placing the beaker in cool water.
4. While continuing to stir, adjust the pH to 7.4 using 5 N NaOH.
5. Using ddH_2O and a graduated cylinder; bring the total volume to exactly 100ml.
6. Store at room temperature. Do not store at 4 °C or the solution will precipitate.

1X PBS Buffer (100ml):

1. Add 5ml of 20X PBS to 95ml of ddH_2O.
2. Invert several times
3. Check that pH is at 7.4, if not adjust using 1N NaOH
4. Store at 4° C for up to two days.

Blocking Solution

0.1 % Triton X
3 % Normal Serum (from the animal the secondary antibody was raised in)
5 % Bovine Serum Albumin
71.9 % 1X PBS

To make 10ml combine the follow ingredients (needs to be vortexed to mix completely:

10µl	Triton X
300µl	Normal Donkey Serum
500µl	Bovine Serum Albumin
9190µl	1X PBS

Primary Antibody

Choline Acetyl Transferase (ChAT)
- *Chemicon International AB 144P Goat X ChAT, store at -20°C*

Optimal dilution 1:200
Dilute in blocking solution.

To make 1ml:

5 µl	ChAT antibody
995µl	Blocking solution

Secondary Antibody

Donkey Anti-Goat Alexa Fluor 555
- *Molecular Probes (Invitrogen) A21432, store at 4°C in dark.*

Optimal dilution 1:400
Dilute in 1X PBS

To make 1ml:

2.5µl	Donkey anti-goat AF555
997.5µl	1X PBS

Procedure:

1. Rinse sections 3 x 5 minutes with 1X PBS in 4 x 6 well tissue culture plate on shaker.
2. Prepare Blocking solution: approximately 1ml per sample.
3. After removing 1X PBS, add 1ml of Blocking solution to each well and incubate for 1 hour at room temperature.
4. Prepare Primary Antibody solution: approximately 1 ml per sample
5. Remove Blocking solution and add 1ml of Primary Antibody solution. Place on shaker at room temperature for 1 hour.
6. Cover tissue culture plate with parafilm and place in 4°C for 48 hours (the longer the sections can be left the better, 24 hours is usually sufficient).
7. After removing Primary antibody solution, rinse sections for 5 x 15 minutes in 1X PBS on shaker at room temperature.
8. Prepare Secondary Antibody solution: approximately 1ml per sample, prepared in absence of light.
9. Incubate in Secondary antibody solution for 1.5 hours at room temperature on shaker. Ensure to cover the tissue culture plate with tin foil as the secondary is light sensitive. ** From this step onwards, ensure that sections are kept in

minimal light as exposure will cause the fluorescence of the secondary antibody to fade **

10. Rinse sections for 5 x 15 minutes with 1X PBS.
11. Mount sections onto slides with a fine-tipped paint brush,
12. Allow sections to air-dry.
13. Coverslip with Vectashield Mounting Medium.
14. Once Vectashield has spread out and covers all sections, seal the coverslip with clear nail-polish.
15. Store slides at 4°C in dark.

Imaging[9]

1. Log into UV Lamp book – make sure to log hours used at start of session, and hours on clock when session is complete.
2. In the following order: turn on UV lamp, camera (top of camera), then open the Meta Vue software package on the computer. Failure to do so in sequence will result in the computer crashing. When finished turn off equipment in reverse order.
3. Ensure that the shutter is closed, and the eye-piece view is selected (as opposed to the camera view; see side of microscope).
4. Place slide under the appropriate objective and select the desired filter cube:
   U-MWU2 wide-band cube filter: Fluoro-Gold (peak excitation: 360nm; emission at 620 – white). Note: the visible light hitting the sections will appear blue; sections will immunofluoresce white.
   U-MWIG wide-band cube filter: Alexa Fluor 555 (peak excitation 555nm; emission at 565nm – red). Note: the visible light hitting the sections will appear green; sections will immunofluoresce red.
5. Select the appropriate objective, focus slides through eye-piece, and then switch view to camera.
6. Through the MetaVue program, select "Acquire" from the tool bar then select "Acquire from CoolSnap" and set the following conditions:
   Acquire Menu: a) Select "Intensity Image"
   b) Adjust "Exposure Time" (1ms)
   Region Menu: Select "Entire Chip"
   Colour Balancing: Select "Image Type" as "Fluorescence"
   Preferences: No need for adjustment
7. Select "Start Focusing"
8. Camera will be taking images every 1ms (selected exposure time). Adjust the following settings prior to acquiring final image:
   a) Select "pseudo colour" on side menu bar of image – if you are imaging an AF555 secondary, choose red; Fluoro-Gold – choose blue.
   b) Acquire Menu: click on "Adjust Digital Contrast Icon" - adjust brightness and contrast to predetermined levels.

[9] Adapted with permission from the thesis of Lori Rose Cunningham (M. Sc.2005, SFU).

9. Once image parameters are set, select "Stop Focus", then "Acquire Image". Once image is acquired close the shutter. ** It is important to close the shutter as over-exposure of sections to UV light will cause photo-bleaching **
10. For the double labelling of sections (e.g. AF555 and Fluoro-Gold), ensure that slide is not moved, and repeat steps 5-10 for the alternate secondary antibody or fluorescent tracer.

Note: Once optimal settings have been decided for Exposure Time, Brightness and Contrast, these values should remain constant when all further imaging is conducted using the corresponding fluorophore-conjugated secondary antibody or fluorescent tracer. This contributes to consistency for comparison of sections throughout the experiment.

Image Overlay

1. On main menu, select "Display" then "Overlay Images"
2. In "Overlay Images Window":
   a) number of images should read 3
   b) select correct source image for each colour of overlay e.g. Fluoro-Gold for blue source, AF555 image for red source. The third source should be grey.
   c) select "Apply Overlay"
3. A new window will appear with your overlaid image.

Saving an Image

1. Save as TIFF file for use within MetaVue software
2. For use with other imaging programs (such as Adobe Photoshop) save file as 8-bit: Select Display from the toolbar then select "Scale Image". On the "Scale Image" menu select "copy to 8-bit image". Once this is done you will have a replica of your full TIFF image but as an 8-bit file vs. a 16-bit file. Save with the appropriate title as both files are saved as .TIFF with no recognizable difference. I.e. Save original TIFF as 130iChAT.TIFF and the 8-bit copy as 130iChAT-8bit.TIFF.

REFERENCES

Alberts B, Bray D, Lewis J, Raff M, Roberts K, and Watson JD. (1994). Molecular Biology of the Cell. 3rd Ed. Taylor & Francis Group: New York, NY. Pages 618-622.

Alexander GM, Erwin, KL, Byers N, Deitch JS, Augelli BJ, Blankenhorn EP, and Heiman-Patterson TD. (2004). Effect of transgene copy number on survival in the G93A SOD1 transgenic mouse model of ALS. *Molecular Brain Research* 130:7-15.

Anderson J. (2003). Defects in dynein linked to motor neuron degeneration in mice. *SAGE KE*, 18:PE10.

Azzouz M, Ralph GS, Storkebaum E, Walmsley LE, Mitrophanous KA, Kingsman SM, Carmeliet P, and Mazarakis ND. (2004) VEGF delivery with retrogradely transported lentivector prolongs survival in a mouse ALS model. *Nature* 429:413-417.

Beckman JS, Carson M, Smith CD, Koppenol WH. (1993). ALS, SOD, and peroxynitrite. *Nature* 364:584.

Bennett MR, McGrath PA, Davey DF, and Hutchinson I. (1983). Death of motorneurons during the postnatal loss of polyneuronal innervation of rat muscles. *J Comp Neurol* 218:351-363.

Bisby MA. (1977). Retrograde axonal transport of endogenous protein: differences between motor and sensory axons. *J Neurochem* 28:249-251.

Bjornskov EK, Norris FH Jr, and Mower-Kuby J. (1984). Quantitative axon terminal and end-plate morphology in amyotrophic lateral sclerosis. *Arch Neurol* 41: 527-530.

Boillee S & Cleveland DW. (2004). Gene therapy for ALS delivers. *TRENDS in Neuroscience* 27(5):235-238.

Bommel H, Xie G, Rossoll W, Wiese S, Jablonka S, Boehm T, and Sendtner M. (2002). Missense mutation in the tubulin-specific chaperone E (Tbce) gene in the mouse mutant progressive motor neuronopathy, a model of human motoneuron disease. *J Cell Biol* 159:563-569.

Borasio GD. (1998). A placebo-controlled trial of insulin-like growth factor-I in amyotrophic lateral sclerosis. European ALS/IGF-I Study Group. *Neurology* 51:583-586.

Brown RH Jr. (1995). Amyotrophic Lateral Sclerosis: recent insights from genetic and transgenic mice. *Cell* 80:687-692.

Brownell B, Oppenheimer DR, and Hughes T. (1970). The central nervous system in motor neurone disease. *J Neurol Neurosurg Pscychiatry* 33:338-357.

Bruijn LI, Houseweart MK, Kato S, Anderson KL, Anderson SD, et al. (1998). Aggregation and motor neuron toxicity of an ALS-linked SOD1 mutant independent from wild-type SOD1. *Science* 281:1851-1854.

Bruijn LI, Miller TM, and Cleveland DW. (2004). Unraveling the mechanisms involved in motor neuron degeneration in ALS. *Annu Rev Neurosci* 27:723-749.

Burgess SA, Walker ML, Sakakibara H, Knight PJ, and Oiwa K. (2003). Dynein structure and power stroke. *Nature* 421:715-718.

Camu W, Khoris J, Moulard B, Salachas F, Biolotti V, Rouleau G, and Meininger V. (1999). Genetics of familial ALS and consequences for diagnosis. French ALS research group. *J Neurol* 165 (Suppl1):S21-26.

Chiu AY, Zhai P, Dal Canto MC, Peters TM, Kwon YW, Prattis SM, and Gurney ME. (1995). Age-dependent penetrance of disease in a transgenic mouse model of familial amyotrophic lateral sclerosis. *Neurosci* 6:349-362.

Cleveland DW, Laing N, Hurse PV, and Brown RH. (1995). Toxic mutants in Charcot's sclerosis. *Nature* 378:342-343

Collard J-F, Cote F and Julien J-P. (1995). Defective axonal transport in a transgenic mouse model of amyotrophic lateral sclerosis. *Nature* 375:61-64.

Connolly JL, Greene LA, Viscarello RR, and Riley WD. (1979). Rapid, sequential changes in surface morphology of PC12 pheochromocytoma cells in response to nerve growth factor. *J Cell Biol* 82:820-827.

Crews LL and Wigston DJ. (1990). The dependence of motoneurons on their target muscle during postnatal development of the mouse. *J Neurosci* 10:1643-1653.

Cunningham LR. (2005). Increased skeletal muscle Akt content in a murine model of motor neuron disease. *SFU Thesis.*

Czlonkowska A, Ciesielska A, Gromadzka G, and Kurkowska-Jastrzebska I. (2005). Estrogen and cytokines production – the possible cause of gender differences in neurological diseases. *Curr Pharm Design* 11:1017-1030.

Dal Canto MC and Gurney ME. (1995). Development of central nervous system pathology in a murine transgenic model of human amyotrophic lateral sclerosis. *Am J Path* 145(6):1271-1279.

de Belleroche J, Orrell R, and King A. (1995). Familial Amyotrophic Lateral Sclerosis/motor neurone disease (FALS): a review of current developments. *J Med Genet* 32:841-847.

Deinhardt K and Schiavo G. (2005). Endocytosis and retrograde axonal traffic in motor neurons. *Biochem Soc Symp* 72:139-150.

Delisle MB & Carpenter S. (1984). Neurofibrillary axonal swelling and amyotrophic lateral sclerosis. *J Neurol Sci* 63:241-250.

Eisen A & Krieger C. (1998). Amyotrophic Lateral Sclerosis: synthesis of research and clinical practice. Cambridge University Press: New York, NY.

Eisen A, Pearmain J, and Stewart H. (1995). Dehydroepiandrosterone sulphate (DHEAS) concentrations and amyotrophic lateral sclerosis. *Muscle & Nerve* 18:1482-1483.

Feeney SJ, McKelvie PA, Austin L, Jean-Francois MJ, Kapsa R, Tombs SM, and Byrne E. (2001). Presymptomatic motor neuron loss and reactive astrocytosis in the SOD1 mouse model of Amyotrophic Lateral Sclerosis. *Muscle & Nerve* 24:1520-1519.

Fischer LR, Culver DG, Tennant P, Davis AA, Wang M et al. (2004). Amyotrophic lateral sclerosis is a distal axonopathy: evidence in mice and man. *Exper Neurol* 185:232-240.

Forger NG, Hodges LL, Roberts SL, and Breedlove SM. (1992). Regulation of motoneuron death in the spinal nucleus of bulbocavernosus. *J Neurobiol* 23:1192-1203.

Frey D, Schneider C, Xu L, Borg J, Spooren W, and Caroni P. (2000). Early and selective loss of neuromuscular synapse subtypes with low sprouting competence in motoneuron diseases. *J Neurosci* 20:2534-2542.

Fullerton HJ, Ditelberg JS, Chen SF, Sarco DP, Chan PH, Epstein CJ, and Ferriero DM. (1998). Copper/zinc superoxide dismutase transgenic brain accumulates hydrogen peroxide after perinatal hypoxia ischemia. *Ann Neurol* 44:37-364.

Gong YH & Elliot JL. (2000). Metallothionein expression is altered in a transgenic murine model of familial amyotrophic lateral sclerosis. *Exp Neurol* 162:27-36.

Glover JC. (2000). Development of specific connectivity between premotor neurons and neurons in the brainstem and spinal cord. *Physiol Rev* 80:615-647.

Gonzalez de Aguilar JL, Dupuis L, Oudart H, and Loeffler JP. (2005). The metabolic hypothesis in amyotrophic lateral sclerosis: insights from Cu/Zn-superoxide dismutase mice. *Biomed Pharmacother* 59:190-196.

Gurney ME. (1994). Transgenic-mouse model of amyotrophic lateral sclerosis. *N Engl J Med* 331:1721-1722.

Gurney ME. (1997). The use of transgenic mouse models of amyotrophic lateral sclerosis in preclinical drug studies. *J Neurol Sci* 152(Suppl. 1):S67-S73.

Gurney ME, Tomasselli AG, and Heinrikson RL. (2000). Stay the executioner's hand. *Science* 288 (5464):283-285.

Hadano S, Hand CK, Osuga H, Yanagisawa Y, Otomo A, et al. (2001). A gene encoding a putative GTPase regulator is mutated in familial amyotrophic lateral sclerosis. *Nat Genet* 29:166-173.

Haenggeli C & Kato AC. (2002). Rapid and reproducible methods using Fluorogold for labelling a subpopulation of cervical motoneurons: application in the wobbler mouse. *J Neurosci Methods* 116:119-124.

Hafezparast M, Klocke R, Ruhrberg C, Marquardt A, Ahmad-Annuar A, et al. (2003). Mutations in dynein link motor neuron degeneration to defects in retrograde transport. *Science* 300:808-812.

Hand CK and Rouleau GA. (2002). Familial Amyotrophic Lateral Sclerosis. *Muscle & Nerve* 25:135-159.

Haverkamp LJ, Appel V, and Appel SH. (1995). Natural history of amyotrophic lateral sclerosis in a database population. Validation of a scoring system and a model for survival prediction. *Brain* 118:707-719.

Heerssen HM, Pazyra MF, and Segal, RA. (2004). Dynein motors transport activated Trks to promote survival of target-dependent neurons. *Nat Neurosci* 7:596-604.

Hirokawa N. (1998). Kinesin and dynein superfamily proteins and the mechanism of organelle transport. *Science* 279:519-526.

Hirokawa N, Sato-Yoshitake R, Yoshida T, and Kawashimea T. (1990). Brain dynein (MAP1C) localizes on both anterogradely and retrogradely transported membranous organelles in vivo. *J Cell Biol* 111:1027-1037.

Hu JH, Chernoff K, Pelech S, and Krieger C. (2003). Protein kinase and protein phosphatase expression in the central nervous system of G93A mSOD over-expressing mice. *J Neurochem* 85(2):322-331.

Jaarsma D, Hassdijk ED, Grashorn JA, Hawkins R, van Duijn W, et at. (2000). Human Cu/Zn superoxide dismutase (SOD1) overexpression in mice causes mitochondrial vacuolization, axonal degeneration, and premature motor neuron death and accelerates motoneuron disease in mice expressing a familial amyotrophic lateral sclerosis mutant SOD1. *Neurobiol Dis* 7:623-643.

Jablonka S, Wiese S, and Sendtner M. (2004). Axonal defects in mouse models of motoneuron disease. *J Neurobiol* 58:272-286.

Joseph DR, O'Brien DA, Sullivan PM, Becchis M, Tsuruta JK, and Petrusz P. (1997). Overexpression of androgen-binding protein/sex hormone binding globulin in male transgenic mice: tissue distribution and phenotypic disorders. *Biol Reprod* 56:21-32.

Ju G, Han ZS, and Fan LZ. (1989). Fluorogold as a retrograde tracer used in combination with immunohistochemistry. *J Neurosci Methods* 69:69-72.

Kaspar BK, Llado J, Sherkat N, Rothstein JD and Gage FH. (2003). Retrograde viral delivery of IGF-1 prolongs survival in a mouse ALS model. *Science* 301:839-842.

Kennel PF, Finiels F, Revah F, and Mallet J. (1996). Neuromuscular function impairment is not caused by motor neuron loss in FALS mice: an electromyographic study. *Neuroreport* 7:1427-1431.

Kieran D, Hafezparast M, Bohnert S, Dick JRT, Martin J et al. (2005). A mutation in dynein rescues axonal transport defects and extends the life span of ALS mice. *J Cell Biol* 169:561-567.

Kong J and Xu Z. (1998). Massive mitochondrial degeneration in motor neurons triggers the onset of amyotrophic lateral sclerosis in mice expressing a mutant SOD1. *J Neurosci* 18:3241-3250.

Kriz J, Nguyen MD, and Julien JP. (2002). Minocycline slows disease progression in a mouse model of amyotrophic lateral sclerosis. *Neurobiol Dis* 10:268-278.

Lai EC, Felice KJ, Festoff BW, Gawel MJ, Gelinas DF, Kratz R, Murphy MF, Natter HM, Norris FH, and Rudnicki SA. (1997). Effect of recombinant human insulin-like growth factor-I on progression of ALS. A placebo-controlled study. The North America ALS/IGF-I Study Group. *Neurology* 49:1621-1630.

LaMonte BH, Wallace KE, Holloway BA, Shelly SS, Ascano J, et al. (2002). Disruption of dynein/dynactin inhibits axonal transport in motor neurons causing late-onset progressive degeneration. *Neuron* 34:715-727.

Lee MK & Cleveland DW. (1996). Neuronal intermediate filaments. *Annu Rev Neurosci* 19:187-217.

Ligon LA, LaMonte BH, Wallace KE, Weber N, Kalb RG, and Holzbaur ELF. (2005). Mutant superoxide dismutase disrupts cytoplasmic dynein in motor neurons. *Neuroreport* 16:533-536.

Ligon LA, Tokito M, Finklestein JM, Grossman FE, and Holzbaur ELF. (2004). A direct interaction between cytoplasmic dynein and kinesin I may coordinate motor activity. *J Biol Chem* 279:19201-19208.

Litchy WJ. (1983). Uptake and retrograde transport of horseradish peroxidase in frog sartorius nerve in vitro. *Brain Res* 56:377-381.

Lowry K, Quach H, Wreford N, and Cheema SS. (2001). There is no loss of motor neurons in the rat spinal cord during postnatal maturation. *J Anat* 198:473-479.

Militello A, Vitello G, Lunetta C, Toscano A, Maiorana G et al. (2002). The serum level of free testosterone is reduced in amyotrophic lateral sclerosis. *J Neurol Sci* 195:67-70.

Millecamps S, Nicolle D, Ceballos-Picot I, Mallet J, and Barkats M. (2001). Synaptic sprouting increases the uptake capacities of motoneurons in amyotrophic lateral sclerosis mice. *PNAS* 98:7582-7587.

Miller RG. (2001). Examining the evidence about treatment of ALS/MND. *Amyotroph Lateral Scler Other Motor Neuron Disord* 2(1):3-7

Miller TM and Cleveland DW. (2003). Has gene therapy for ALS arrived? *Nature Medicine* 9:1256-1257.

Mitsumoto H, Ferut AL, Kurahashi K, and McQuarrie IG. (1990). Impairment of retrograde axonal transport in wobbler mouse motor neuron disease. *Muscle & Nerve* 13:121-126.

Mulder DW, Kurland LT, Offord KP, and Beard CM. (1986). Familial adult motor neuron disease amyotrophic lateral sclerosis. *Neurology* 36:511-517.

Murashov AK, Islamov RR, McMurray RJ, Elena SP, and Weidner DA. (2004). Estrogen increases retrograde labelling of motoneurons: evidence of a nongenomic mechanism. *Am J Physiol Cell Physiol* 287:320-326.

Nagano S, Satoh M, Sumi H, Fujimura H, Tohyama C, et al. (2001). Reduction of metallothioneins promotes the disease expression of familial amyotrophic lateral sclerosis mice in a dose-dependent manner. *Eur J Neurosci* 13:1363-1370.

Oda Y and Nakanishi I. (2000). The distribution of cholinergic neurons in the human central nervous system. *Histol Histopathol* 15(3):825-834.

Pasinelli P, Houseweart MK, Brown RH Jr, and Cleveland DW. (2000). Caspase-1 and -3 are sequentially activated in motor neuron death in Cu, Zn superoxide dismutase-mediated familial amyotrophic lateral sclerosis. *Proc Natl Acad Sci USA* 97:13901-13906.

Peluffo H, Estevez A, BarbeitoL, and Stutzmann JM. (1997). Riluzole promotes survival of rat motoneurons in vitro by stimulating trophic activity produced by spinal astrocyte monolayers. *Neurosci Lett* 228:207-211.

Pérez J & Kelley DB. (1996). Trophic effects of androgen: receptor expression and survival of laryngeal motor neurons after axotomy. *J Neurosci* 16:6625-6633.

Peyronnard J & Charron L. (1983). Decreased horseradish peroxidase labelling in deafferented spinal motoneurons of the rat. *Brain Res* 275:203-214.

Puls I, Jonnakuty C, LaMonte BH, Holzbaur EL, Tokito M, et al. (2003). Mutant dynactin in motor neuron disease. *Nat Genet* 33:455-456.

Reaume AG, Elliot JL, Hoffman EK, Kowall NW, Ferrante RJ, et al. (1996). Motor neurons in Cu/Zn superoxide dismutase-deficient mice develop normally but exhibit enhanced cell death after axonal injury. *Nat Genet* 13:43-47.

Rinamen L, Milligan CE, and Levitt P. (1991). Persistence of fluoro-gold following degeneration of labelled motoneurons is due to phagocytosis by microglia and macrophages. *Neurosci* 44:765-776.

Rosen DR, Dissique T, Patterson D, Figlewicz DA, Sapp P, et al. (1993). Mutations in Cu/Zn superoxide dismutase gene are associated with familial amyotrophic lateral sclerosis. *Nature* 362:59-62.

Rothstein JD, Bristol LA, Hosler B, and Brown RH Jr. (1994). Chronic inhibition of superoxide dismutase produces apoptotic death of spinal neurons. *Proc Natl Acad Sci USA* 91:4155-4159.

Rudnicki SA. (1999). Estrogen replacement therapy in women with amyotrophic lateral sclerosis. *J Neurol Sci* 169:126-127.

Sagot Y, Rosse T, Vejsada R, Perrelet D, and Kato AC. (1998). Differential effects of neurotrophic factors on motoneuron retrograde labeling in a murine model of motoneuron disease. *J Neurosci* 18(3):1132-1141.

Sanes JR, Schachner M, and Covault J. (1986). Expression of several adhesive macromolecules (N-CAM, L1, J1, NILE, uvomorulin, laminin, fibronectin, and heparin sulphate proteoglycan) in embryonic, adult, and denervated adult skeletal muscle. *J Cell Biol* 102:420-431.

Scarisbrick IA, Haase P, and Hrycyshyn AW. (1990). The arrangement of forearm motoneurons in young and adult rats and the possibility of naturally occurring motoneurons death. *J Anat* 171:57-67.

Schmued LC & Fallon JH. (1986). Fluoro-Gold: a new fluorescent retrograde axonal tracer with numerous unique properties. *Brain Res* 377:147-154.

Shaw CE, Enayat ZE, Chioza BA, Al Chalabi A, Radunovic A, Powell JF, and Leigh PN. (1998). Mutations in all five exons of SOD1 may cause ALS. *Ann Neurol* 43:390-394.

Siddique T and Deng HX. (1996). Genetics of amyotrophic lateral sclerosis. *Hum Mol Genet* 5:1465-1470.

Sobue G, Sahashi K, Takahashi A, Matsuoka Y, Muroga T, and Sobue I. (1983). Degenerating compartment and functioning compartment of motor neurons in ALS: possible process of motor neuron loss. *Neurology* 33:654-657.

Strong M and Rosenfeld J. (2003). Amyotrophic Lateral Sclerosis: A review of current concepts. *ALS and other motor neuron disorders* 4:136-143.

Swash M, Leader M, Brown A, Swettenham KW. (1986). Focal loss of anterior horn cells in the cervical cord in motor neuron disease. *Brain* 109:939-952.

Torres-Aleman I, Barrios V, and Berciano J. (1998). The peripheral insulin-like growth factor system in amyotrophic lateral sclerosis and in multiple sclerosis. *Neurology* 50:772-776.

Trieu VN & Uskun FM. (1999). Genistein is neuroprotective in murine models of familial amyotrophic lateral sclerosis and stroke. *Biochem Biophys Res Commun* 258:685-688.

Vallee RB, Williams JC, Varma D, and Barnhart LE. (2003). Dynein: An ancient motor protein involved in multiple modes of transport. *J Neurobiol* 58:189-200.

Van Den Bosch L, Tilkin P, Lemmens G, and Robberecht W. (2002). Minocycline delays disease onset and mortality in a transgenic model of ALS. *Neuroreport* 13:1067-1070.

Vanden Noven S, Wallace N, Muccio D, Turtz A, and Pinter MJ. (1993). Adult spinal motoneurons remain viable despite prolonged absence of functional synaptic contact with muscle. *Experimental Neurology* 128:147-156.

Veldink JH, Bär PR, Joosten EA, Otten M, Wokke JH, and van den Berg LH. (2003). Sexual differences in onset of disease and response to exercise in a transgenic model of ALS. *Neuromuscular Disorders* 13:737-743.

Weiner LP. (1980). Possible role of androgen receptors in amyotrophic lateral sclerosis. A hypothesis. *Arch Neurol* 37:128-131.

Wessendorf MW. (1991). Fluoro-Gold: composition, and mechanism of uptake. *Brain Res* 553:135-148.

Williamson TL and Cleveland DW. (1999). Slowing of axonal transport is a very early event in the toxicity of ALS-linked SOD1 mutants to motor neurons. *Nat Neurosci* 2:50-56.

Williamson TL, Bruijn LI, Zhu Q, Anderson KL, Anderson SD, Julien JP, and Cleveland DW. (1998). Absence of neurofilaments reduces the selective vulnerability of motor neurons and slows disease caused by a familial ALS-linked SOD1 mutant. *Proc Natl Acad Sci USA* 95:9631-9636.

Yamanaka K, Vande Velde C, Bertini E, Boespflug-Tanguy O, and Cleveland DW. (2003). Unstable mutants in the peripheral endosomal membrane component ALS2 cause early onset motor neuron disease. *Proc Natl Acad Sci* 100:16041-16046.

Yuki S, Takenaka T, Kawakami R, Sakai I, and Saito KI. (1996). Control of axonal transport by recombinant human NGF in cultured mouse dorsal root ganglion cells. *Soc Neurosci Abstract* 22:746.

Zang DW, Lopes EC, and Cheema SS. (2005). Loss of Synaptophysin-positive boutons on lumbar motor neurons innervating the medial gastrocnemius muscle of the $SOD1^{G93\,G1H}$ transgenic mouse model of ALS. *J Neurosci Research* 79:694-699.

Zhu S, Stavrovskaya IG, Drozda M, Kim BY, Ona V, et al. (2002). Minocycline inhibits cytochrome c release and delays progression of amyotrophic lateral sclerosis in mice. *Nature* 417:74-78.